Polymer networks with mobile force-applying crosslinks

Mohau Jacob Mateyisi

Thesis presented in partial fulfilment
of the requirements for the degree of
Master of Science
at Stellenbosch University

Supervisor: Prof. Kristian Müller-Nedebock
Co-Supervisor: Mr Leandro Boonzaaier
March 2011

Declaration

By submitting this thesis electronically, I declare that the entirety of the work contained therein is my own, original work, that I am the sole author thereof (save to the extent explicitly otherwise stated), that reproduction and publication thereof by Stellenbosch University will not infringe any third party rights and that I have not previously in its entirety or in part submitted it for obtaining any qualification.

Date: March 2011

Abstract

We construct and study a simple model for an active gel of flexible polymer filaments crosslinked by a molecular motor cluster that perform reversible work while translating along the filaments. The filament end points are crosslinked to an elastic background. In this sense we employ a simplified model for motor clusters that act as slipping links that exert force while moving along the strands. Using the framework of replica theory, quenched averages are taken over the disorder which originates from permanent random crosslinking of network end points to the background. We investigate how a small motor force contributes to the elastic properties of the network. We learn that in addition to the normal elastic response for the network there is an extra contribution to the network elasticity from the motor activity. This depends on the ratio of the entropic spring constant for the linked bio-polymerchain to the spring constant of the tether of the motor.

Opsomming

Ons konstrueer en bestudeer 'n eenvoudige model vir 'n aktiewe netwerk van fleksieble polimeerfilamente wat deur grosse van molekulêre motors aan mekaar verbind word wat omkeerbare werk doen terwyl dit langs die filamente transleer. Die eindpunte van die filamente is aan 'n elastiese agtergrond verbind. In hierdie sin benut ons 'n eenvoudige model vir motorclusters wat as verskuifbare verbindings krag op die filamente tydens beweging kan uitoefen. Nie-termiese wanorde gemiddeldes word geneem oor die wanorde wat deur die lukrake permanente verbindings van netwerk eindpunte aan die agtergrond veroorsaak word. Ons ondersoek hoe 'n klein motorkrag tot die elastiese eienskappe van die netwerk bydra. Ons leer dat daar bo en behalwe die gewone elastiese respons vir die netwerk 'n elastiese bydrae as gevolg van die motors se aktiwiteit voorkom. Dit hang af van die verhouding van die entropiese veerkonstante van die biopolimerketting tot die veerkonstante van die anker van die motor.

Acknowledgments

I would like to express my sincere thanks to my supervisor Prof. Kristian Müller-Nedebock and my co-supervisor Mr. Leandro Boonzaaier. Their simplicity and encouraging words of wisdom kept me motivated through out the MSc project. I am very grateful to my supervisor for his kind support in identifying interesting and sensible questions for this MSc thesis. I am mostly grateful to him for giving me a chance to enjoy trying things on my own and for having his door open when his guidance was mostly needed. The research tools he introduced me to in the course of this project and his style of asking physics questions, were so enriching and I feel indebted to him. I am also very thankful to my co-supervisor for the fruitful discussions on the technical as well as on the calculational aspect of work. His regular imputs into this work are highly valued.

I feel so privileged for having received financial support from the African Institute for Mathematical Sciences (AIMS) and Stellenbosch University, administrated through the Stellenbosch International Office. This helped me to focus on the academic priorities and I am very thankful for that.

Members of the physics department, fellow students, especially member of the AIMS alumni were very instrumental in making my stay in Stellenbosch homely. Special thanks goes to the members of Active-gels journal club for the fruitful academic exchanges.

I would like to give my heart felt thanks to my wife for her unconditional love and support. Her patience, as I dedicate most of my time to this thesis, is highly appreciated. My parents and relatives' support kept me going, regardless of challenges life presented, a special vote of thanks goes to them.

Last and most importantly, I would like to thank the Almighty God for the life he gave me and for blessing every little effort directed to this work.

Contents

List of Figures

Chapter 1

Introduction

1.1 Mechanical Properties of Active Networks

The understanding of mechanical properties of active networks is important for describing the functioning of a range of biological materials. In eukaryotic cells, mechanical properties are in control of functions such as sensing, force generation, cell motility and cell division [30]. It is a well known fact in the cell biology literature [1,21] that the response of a cell to mechanical stimuli is mediated by the cytoskeleton [18], which is a network of semiflexible filaments linked by a variety of passive and active linkers. This network is predominantly out of equilibrium due to the active processes that lead to network segment formation and crosslinking [23]. The consumption of energy from the hydrolysis of adenosine triphosphate (ATP) into adinosine diphosphate (ADP) keeps the active networks predominantly out of equilibrium. This is a process characteristic of living systems, and it presents a new feature that is not typical of traditional soft matter.

The experimental techniques for studying cellular mechanics are well developed. Forces can be probed at cellular and subcellular level. Under experimental conditions, the location as well as the dynamics of cytoskeleton protein network components during cell processes, such as division, can be observed with great temporal and spatial precision [35]. The most distinctive features of subcellular network architecture and functioning are predetermined by their mechanical stiffness, dynamics of their assembly, polarity and the type of molecular motors with which they associate. A theory explaining the experimentally observed

mechanical properties mediated by the cytoskeleton components is far from complete. This presents an interesting challenge to theoretical physics and this calls for rigorous theoretical consideration. More importantly, non equilibrium processes observed in biological system, such as in cytoskeleton functioning, stand a chance to give rise to new theoretical concepts and ideas.

The central goal of the thesis is to develop a semi-microscopic model that can yield insights into the role played by the force generation of molecular motor crosslinking proteins in the elasticity of active biopolymer networks in the gel phase.

The approach here is to make a careful development on the well known and well established equilibrium network theory methods, commonly used for networks in soft matter systems, such as those invented for study of rubber elasticity [6]. The basic ingredients for the network model we develop are the main cytoskeleton network components. These are biopolymer chains, frequently actin strands in real systems, connected by active crosslinkers called molecular motor clusters that are responsible for reversible forces. Features of the network crosslinkers such as progressivity and force generation are incorporated using biased slip link model. As we shall see in chapter 3, this can be modelled as an equilibrium polymer network model with some annealed and quenched degrees of freedom.

The main model calculation that this thesis is concerned with is a simplified model in which we think of the network in the context of a two stranded network model. The most extreme simplification is that we treat the system in equilibrium statistical physics. The model calculation is preceded by some more simplified or reduced toy model calculations exploring specific aspects of the two strand model. Finally, the insights obtained are used to guide the two strand model calculation. The reduction is achieved by embodying other components of the two strand network by a macroscopic entity (fluid medium) which presents no other interaction other than an effective coupling background. Throughout the work, the reduced model version is referred to as "single stranded network".

The thesis is divided into four chapters:

- In this first chapter, biological details of the network and how they are mathematically parameterised, is presented.

- The initial model calculation presented is that of a one dimensional single stranded network. We derive analytical expressions for internal tension on the connected strands. This forms the material for the second chapter.
- In the third chapter, two model calculations are presented. The first model construction is similar to that of chapter 2 but with system disorder. Presented in the last part of chapter three, is the two strand model constructed in such a way that it is symmetrical about the two connected strands. For both constructions the free energy and the elasticity modulus are derived.
- The fourth chapter is reserved for summary of the results and an outlook on how the model ideas could be extended.

1.2 Bio-polymer Networks

Before mathematically modelling the active biopolymer network, we review key features that are responsible for the observed network mechanical properties. The main focus is placed only on subcellular components that constitute building blocks of active networks. Most of the chemical and biological details of active biopolymer network components, are covered in great detail in the chemistry and biology literature [1, 21]. However, for completeness, and in order to make the underlying basis of our modelling assumptions clear from the outset, this section is dedicated to introducing each network component.

The main components of biological networks are microtubules or actin filaments and molecular motors. Within a cell environment these components are organised into a cytoskeleton which physically and bio-chemically connects the cell to the external environment [22]. The cytoskeleton mediates forces, enabling movement, cell division and changes of cell shape [30]. To perform all these, the cytoskeleton undergoes dynamic and adaptative processes with the component polymers together with the regulatory proteins remaining in constant flux [9].

Microtubules: These are stiff filamentous molecules that can assemble and diassemble dynamically [16,32]. The theory behind their assembly is still yet to be understood. Single microtubules can form relatively linear tracks that extend to about the length of a typical

animal cell. They are fairly stiff (persistence length on the order of mm). The ability of microtubules to dynamically switch between stably growing and rapidly shrinking enables them to search for cellular space quickly [15].

Actin filaments: These are filamentous molecules that are less rigid as compared to macrotubules. Actin filaments elongate steadily in the presence of nucleotide-bound monomers. This is a process that is well suited to produce sustained forces that are required to advance the leading edge of a cell in response to signals that guide chemotaxis [27]. Filopodial protrusion observed in chemotaxis is supported by these bundles of aligned filaments [14]. Their assembly is promoted by a high concentration of crosslinkers that bind to actin filaments bringing about an assembly of highly organised stiff structures [3,31], which include among others, isotropic networks. Experiments show that cell deformability appears to be regulated by the actin cytoskeleton [25].

Molecular motors: These play a fundamentally important role in crosslinking and organising microtubules and actin cytoskeletons [3], for example, myosin motors act on bundles of aligned actin filaments in stress fibers helping cells to contract and to sense their external environment [5, 17]. One of our primary aims is to come up with a model which depicts the role played by molecular motor activity on the elasticity of bio-polymer networks that are well into gelation. Motors also play several roles in intracellular motility for instance, certain types of motors carry cargoe between intracellular compartments and microtubule tracks [36].

1.2.1 Active-gels as description of Actin-myosin Network

From a polymer physics perspective, a cytoskeleton joined together at a number of connecting sites by active as well as fixed crosslinkers (schematically shown in FIG. 1.1), can be thought of as a gel. This kind of gel is termed "active-gel" due to the fact that the crosslinking molecular motors can generate force and do mechanical work. Gels can have either temporary crosslinks (physical gel) or permanent cross-links (chemical) gel [8] depending on the lifetime of the association between the crosslinking proteins and actin in comparison to the experimental time scales. We shall think of the active gels under consideration as physical gels owing to the fact that the crosslink formation results from

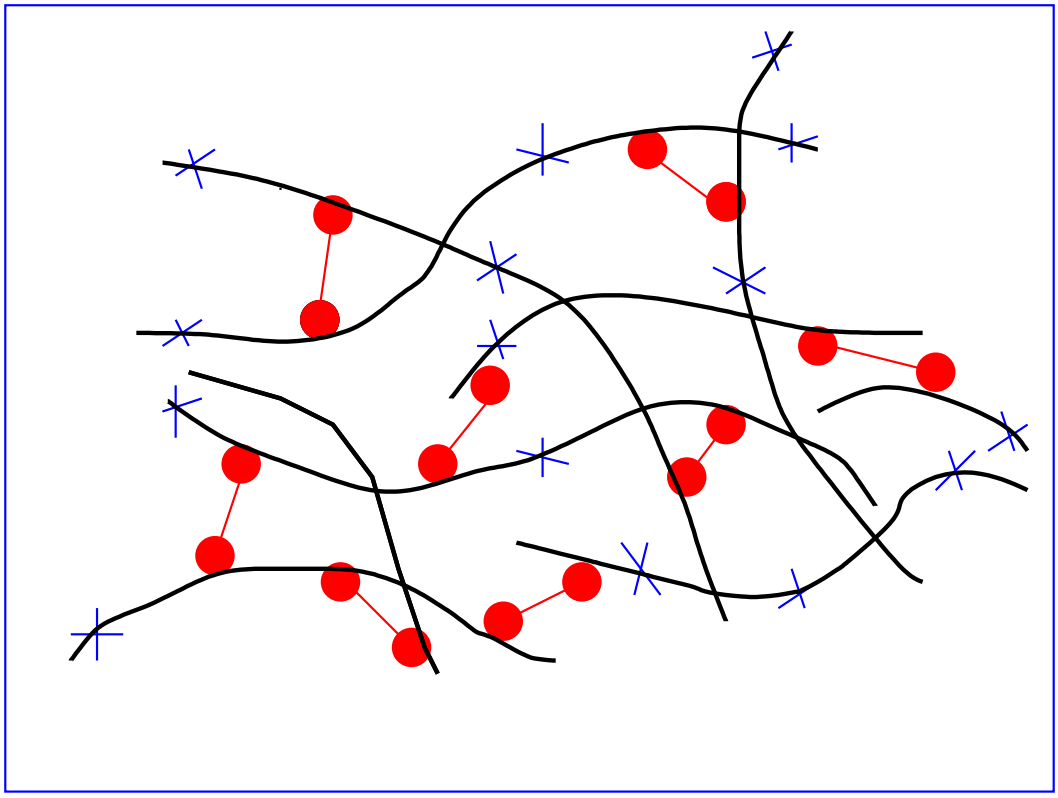

FIG. 1.1. The gel consists of a network of flexible bio-polymer filaments (black coloured strands), placed in a non fluctuating fluid like background which provides anchoring to the network strands. The strands are fixed crosslinked to the background. Crosslinking position per strand (blue crosses) are at fixed separation per realization of the network. The molecular motors clusters active heads (red coloured) are connected by a tether and each of the active motor heads is crosslinked to a filament. The motors are energetically biased along the network strands and they can slip along the the strands

a physical interaction between actin filaments and molecular motors. If the crosslinking process occur quickly, it is possible to make a gel with a very uniform network [1]. On account of this, in network model calculations, instantaneous crosslinking assumption is often used. This makes it possible to do calculations without having to worry about network uniformities.

Real active networks observed in living systems, undergo dynamical and nonequilibrium changes in structure. A general description of this kind of active systems can be built based

[1]The structure of the gel differs with the method of crosslinking. This leads to some subtleties in theoretical as well as experimental studies of gels

on dynamical theory[2] with features such as force balance reflected [26]. An alternative approach which appears to be useful is the so-called hydrodynamic theory [20,24]. This works only for large time scales and long length scales[3]. This turns out to be disadvantageous as not all parameters of the system could be determined directly with this method. The method has to be complemented either by experiments or semi-microscopic theory.

Here, we formulate an active network theory from an equilibrium perspective. We adopt some well established methods [6] commonly used in equilibrium network theory to fit non equilibrium networks. Brute as the approach may appear at first sight, we shall demonstrate that it is capable of accounting for some observed elasticity of active networks subject to deformation. In essence, this is a thermodynamic approach based on the free energy minimization. The approach is more relevant for the static case when the polymerization and depolymerization of individual polymer strands is balanced or at short time scales, as compared to polymerization and depolymerization time scales for constituent biopolymers.

We start by introducing the statistical properties of flexible polymer chains which are important in the construction of the network models and we also demonstrate how material properties of flexible polymer networks are mathematically parametrised. Although cells' cytoskeletal filaments are known to be semi-flexible, we shall think of them as Gaussian polymers. The results of the treatment of network segments as Gaussian flexible polymers at most experimental setups are generic due to the fact that at lower resolutions (micrometer scale) polymer chains become equivalent to each other and exhibit common behavior.

1.3 Modelling Network Segments

The purpose of this section is to take the reader through a brief tour of the theory behind mathematical and statistical models commonly used for mathematically abstracting flexible polymer networks. The details presented are found in the literature published since the

[2]In order to model the system, one can can first write the microscopic equations for actin filaments with the molecular machines and then coarse grain them to a macroscopic or mesoscopic scale where mechanical properties of the network can be studied.

[3]In an active gel, for instance, the hydrodynamic theory can describe properties of gels at length scales bigger than the mesh size.

latter half of the last century. Therefore, it will be necessary to dedicate to this section only aspects of the theory which shall be used as building blocks for the problems that this thesis is concerned with.

1.3.1 Properties of Network Connected Strands

In general, a number of features have to be considered when modelling networks in soft matter systems. The first is chain flexibility. Chains may oppose strong bending (stiff chains) or chains may be highly flexible, hence they are prone to coiling. To parameterise chain flexibility, use is made of the orientational correlation function $k_{or} = \langle \hat{e}(l)\hat{e}(l + \Delta l)\rangle$ which describes the correlation between the chain direction at two points with are at a curvilinear distance Δl from each other. The unit vector $\hat{e}(l)$ denotes the varying local chain direction. $<\cdot>$ indicates an ensemble average over all chain conformations. For sufficiently large distance Δl, the orientational correlation must vanish due to flexibility. As for a parameter that measures the chain stiffness, a suitable choice mostly used in the literature, which we shall use, is the persistence length:

$$\ell_p = \int_0^\infty k_{or}(\Delta l) d(\Delta l), \tag{1.1}$$

which can be expressed simply as the integral over the correlation function. However, throughout the thesis we shall model the network segments as Gaussian. The Gaussian model is a basic model in which the chains are considered to possess no bending rigidity and we shall use it for mathematical simplicity.[4] It is relevant for actin networks when the crosslinked chains are considered large compared to the persistence length. The model assumes that chain segments could be described in terms of their statistical mean. Specifically, to deduce chain conformations, a chain is split into subchains of uniform length, but of length longer than the persistence length ℓ_p. A sequence of vectors, $\{\Delta \mathbf{r}_n\} = (\mathbf{r}_1 - \mathbf{r}_2, \mathbf{r}_3 - \mathbf{r}_2, \cdots \mathbf{r}_N - \mathbf{r}_{N-1})$, is associated such that, the vectors connect the junction points of the subchain. Equivalently the chain conformations could be described by a set of position vectors $\{\mathbf{r}_n\} = (\mathbf{r}_1, \mathbf{r}_2, \cdots, \mathbf{r}_n)$. This is a segmental chain consisting of N units. The global properties of the chain shall be described by considering the distribution function of the segments of the chains.

[4] Inclusion of persistence a project for the future.

One quantity of interest is the end-to-end vector, a vector connecting the two ends of the chain. The chain can be divided into n linked subchains. The end-to-end vector of the chain can be expressed in terms of the end-to-end vector of the sub-chains written as $R = \Sigma_{n=1}^{N} \Delta \mathbf{r}_n$. When the sub-chains are large compared to the persistence length, the successive steps $\Delta \mathbf{r}_n$ of the sub-strands of the chain are orientationally uncorrelated. Therefore, their movement is analogous to Brownian motion and their distribution $\psi(\Delta \mathbf{r}_n)$, is Gaussian. In a similar manner the position vectors $\mathbf{r}_n$ become independent of each other and the conformation distribution function of the chain is given by

$$\psi\left\{\mathbf{r}_n\right\} = \prod_{n}^{N} \left[\frac{3}{2\pi l^2}\right]^{\frac{3}{2}} e^{-\frac{3r_n^2}{2l^2}}, \tag{1.2}$$

where l is called the Kuhn length. We can think of the chains as consisting of beads see (FIG. 1.2) with each bead interacting only with its subsequent neighbour via a potential of the form,

$$U(\mathbf{R}_n) = \frac{3k_B T}{2l^2} \sum_{n=1}^{N} (\mathbf{r}_n - \mathbf{r}_{n-1})^2. \tag{1.3}$$

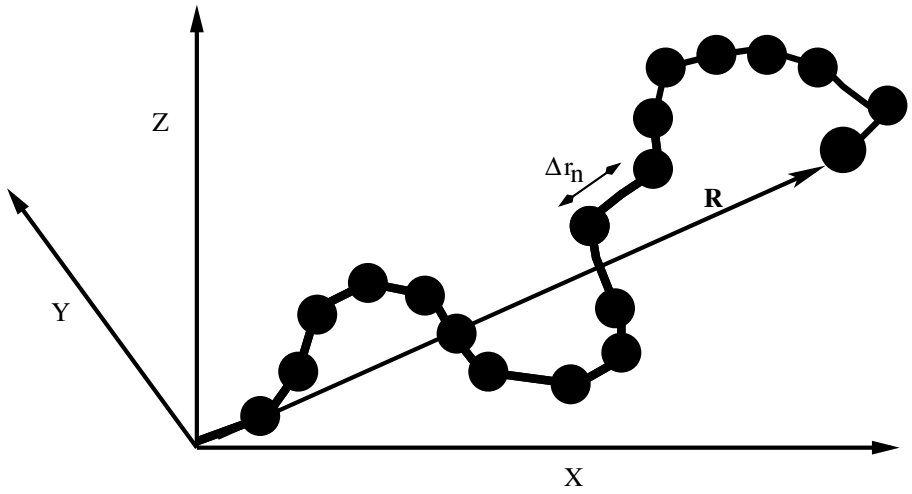

FIG. 1.2. Bead-Spring model for Gaussian polymer chain

The spring constant for each bond is temperature dependent and is given by $\frac{3k_B T}{2l^2}$. The subscript n of the chain is often taken to be a continuous viariable [7], in which case

$\mathbf{r}_n - \mathbf{r}_{n-1} \rightarrow \frac{\partial \mathbf{R}_n}{\partial n}$, leading to

$$\psi[\mathbf{R}_n] = \text{const} \times \left[\exp\left(-\frac{3}{2l^2} \int dn \left(\frac{\partial \mathbf{R}_n}{\partial n} \right)^2 \right) \right]. \tag{1.4}$$

Considering the case where the chain is extending from the position $\mathbf{r}$ to some other position, say $\mathbf{r}'$. The partition function is the Wiener path integral expressed as

$$G(\mathbf{r}, \mathbf{r}'; N) = \int_{R(0)=\mathbf{r}}^{R(s)=\mathbf{r}'} [DR] \exp\left(-\frac{3}{2l^2} \int_0^N \left(\frac{\partial \mathbf{R}_n}{\partial n} \right)^2 dn \right), \tag{1.5}$$

[7] which is a solution of the differential equation of the type,

$$\left[\frac{\partial}{\partial N} - \frac{l^2}{6} \frac{\partial^2}{\partial \mathbf{r}^2} \right] G(\mathbf{r}, \mathbf{r}'; N) = \delta(\mathbf{r} - \mathbf{r}')\delta(N). \tag{1.6}$$

It can be shown with ease that

$$G(\mathbf{r}, \mathbf{r}'; N) = \left(\frac{3}{2\pi l^2 N} \right)^{\frac{3}{2}} \exp\left(-\frac{3}{2\ell^2} \frac{(\mathbf{r} - \mathbf{r}')^2}{N} \right). \tag{1.7}$$

1.3.2 Gaussian Chain and Interaction

Actin filaments are know to have polarity [1], therefore it should be expected that there is dipole interaction on the constituent molecules. The Gaussian chain does not correctly describe the local structure of the actin polymer stands owing to the fact that Gaussian chains assume statistical independence of adjacent bonds which is not generally true for most polymers due to short range interactions. However, the Gaussian chain does describe correctly the structure at long length scales since for most polymers the bond-to-bond correlation decreases rapidly with the separation between bonds along the polymer chain. Although this mechanical Gaussian chain model effectively describes polymer chains with interaction existing between neighboring monomers along the same polymer chain, it does not account for dipole interactions that may exist between monomers separated far apart on the same polymer chain and excluded volume interactions. In classical network theories [4], such interaction are added to the mesoscopic hamiltonian by hand. In this work, to keep the mathematical description simple, we ignore such interactions altogether. The chains are considered to be phantom in nature. In our models, the polarity of the monomers feature only in the biasing nature of the active crosslinks.

1.3.3 Slip Link Model

For modelling mobile active crosslinks we use, as a basis, the so called slip link model [4]. Slip link models were invented to treat network defects called entanglements, [2, 11, 12] in the development of the theory of rubber elasticity. Entanglements occur beyond a certain polymer chains concentration when polymer segments begin to overlap. For a schematic view of entanglements see FIG 1.3(a). In this work the polymer chains are assumed to be non-overlapping and entanglements are ignored. The central feature of slip link models, which we take advantage of, is a degree of freedom along the connected strands. In classical network theory a slip link is modelled as a ring, see FIG. 1.3(b). The ring constrains two polymer strands running through it to stay adjacent to one another.

We model active crosslinks as active slip links. Active slip links, like normal slip links, constrain one polymer to stay adjacent to one another. The departure of active slip links from normal slip links, is that they exert forces resulting from activity. The forces are biased due to the fact that the actin strands are polar. Making the biasing force reversible allows an equilibrium statistical physics treatment. This is a rough model in which a molecular motor cluster tether is modeled as a spring connecting the two active domains, see FIG. 1.3(c). The slipping nature of the crosslink captures the fact that non progressive motors such as myosin motors become progressive once in a cluster. Although, this treatment ignores certain microscopic details of the network components, such as the finer details of the collective behaviour of motor clusters [19], it is powerful enough to capture some desired features of the system using as few effective parameters as possible.

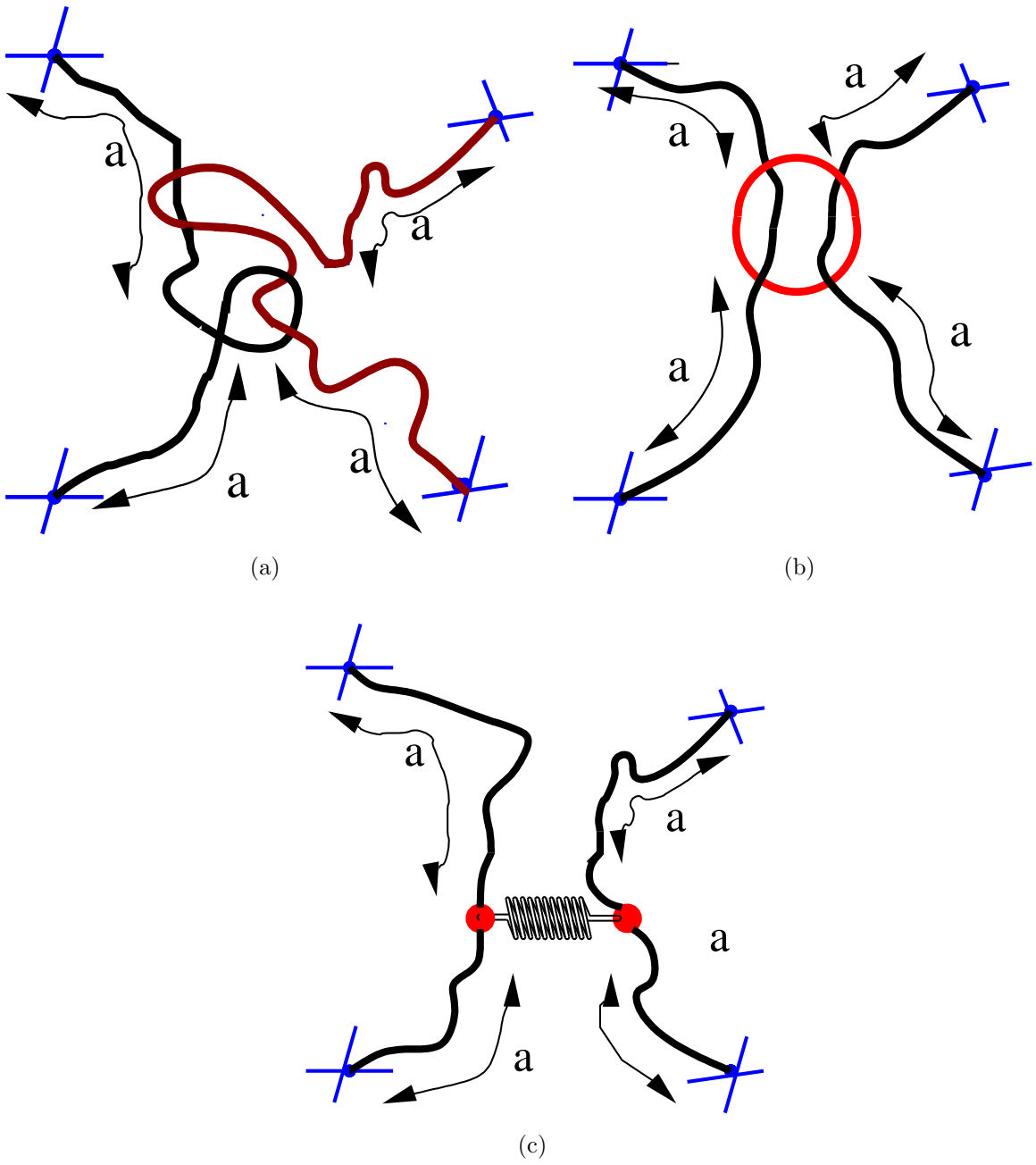

FIG. 1.3. The figure shows a schematic diagram of entanglements in a simple network of two strands 1.3(a), subfigure 1.3(b) is a slip link model in which the entanglement is modelled as by a ring (shown in red) that can slide along the connected strands [4]. Subfigure 1.3(c) shows our slipping active cross link model construction for molecular an actively crosslinked network. Shown in red are the active motor cluster binding domains. The tether connecting the domains is modelled as a spring. a in the above diagrams is a degree of freedom along the connected strands for the slipping component of the network.

Chapter 2

Reduced Two Strand Model

As shown in FIG 1.1, a typical active gel with active crosslinks consist of semiflexible chains crosslinked in a variety of ways. In this chapter we present a considerably simplified network model in which we consider only a single strand attached between fixed points crosslinked to a molecular motor cluster that introduce a biasing force on the network strands, see FIG. 2.1. We model the network strand as flexible chains. The free energy for the system is calculated for different extension regimes and the effect of motor activity on the network internal tension is also derived.

2.1 Model description

Our model consists of an actin strand which is treated as flexible polymer chain that is attached to some fixed positions at the far ends of the strands such that the end points are at a distance X apart. A molecular motor cluster is crosslinked to the strand at some intermediate position ζ effecting a biasing force f on the strand as it translate on the strand by an arc length $\Delta\sigma$. The other motor domain is crosslinked to the background but at a point intermediate to the chain ends. The tether connecting the motor active domains is modelled as an elastic spring of stiffness k. See FIG.2.1.

The statistical weight including the chain configurations is proportional to $\exp(-\beta H)$ where

H is the Wiener measure which accounts for the connectivity given by

$$H = \frac{3k_BT}{2\ell}\sum_{i=1}^{2}\int_0^{L_i} d\sigma_i \left(\frac{\partial \mathbf{r_i}}{\partial \sigma_i}\right)^2. \tag{2.1}$$

where the arc coordinate $\sigma_i \in [0, L]$ and $L = L_1 + L_2$. k_B is Boltzmann constant and T is the

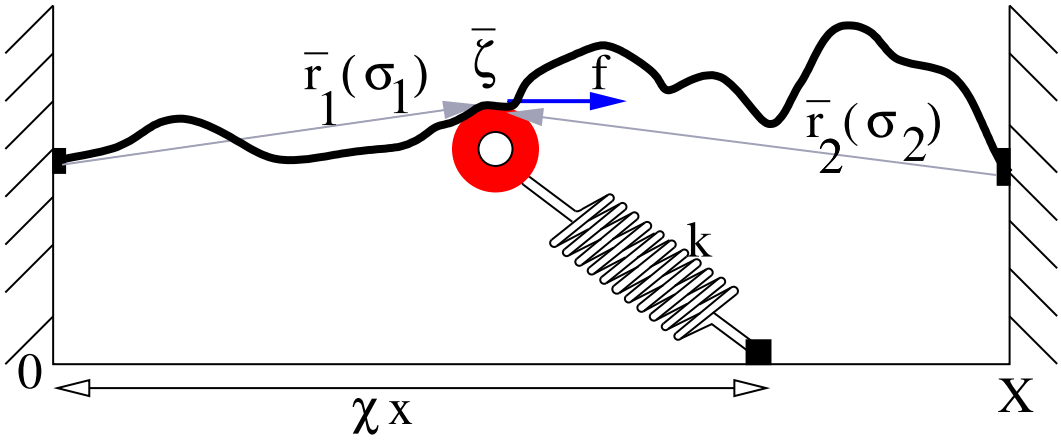

FIG. 2.1. A diagram showing an active network consisting of a single strand crosslinked by some fixed crosslinks, one crosslinker is at the origin and the other at an distance X from the origin. A molecular motor cluster binding head actively crosslink the strand at some position ζ, but capable of slipping along the strand. The other domain of the motor cluster is crosslinked to the background at some position χX, where the slipping parameter $\chi \in [0, 1]$. The tether connecting the motor domains is modelled as a spring of strength k. In the presence of ATP the molecular motor cluster can do work given by $w = \pm f\Delta\sigma_1$, in deforming the strands. The binding motor heads are capable of slipping along their anchoring positions

temperature and ℓ is the kuhn length. The constituent chain segments are parameterised by a position vectors $\mathbf{r}_i(\sigma_i)$. When the molecular machines are active, they can do work $W = \pm f\Delta\sigma_1$ where the variable $\Delta\sigma$ is the degree of freedom directly associated with the molecular motor activity activity via the force f. and $\pm$ account for the polarity of the strands. The energetic contribution of the spring is given by Hooke's law $E = \frac{k}{2}(\boldsymbol{\zeta} - \chi\mathbf{X})^2$, where χ is a parameter, chosen at some value in the interval $[0, 1]$, that determines the attachment position of other motor domain to the background, relative to the extension $\mathbf{X}$ between the fixed crosslinks. The network can be thought of as constituted by two chains of Length L_1 and L_2 being crosslinked by the molecular motor cluster forming a network strand of effective length $L = L_1 + L_2$. The Hamiltonian incorporating all the energetic

contributions to the system is given by

$$H = \frac{3k_BT}{2\ell}\sum_{i=1}^{2}\int_0^{L_i}\partial\sigma_i\left(\frac{\partial\mathbf{r}_i}{\partial\sigma_i}\right)^2 + \frac{k(\zeta-\mathbf{X}\chi)^2}{2} + f\Delta\sigma_1. \tag{2.2}$$

The partition function for the system summing over all possible conformations including all constraints becomes

$$\begin{aligned}\mathcal{Z} &= \int_V d^3\zeta\int_{-\sigma_i}^{L-\sigma_i}d\Delta\sigma_i\int_V[d\mathbf{r}_1]\int_V[d\mathbf{r}_2]e^{-\frac{3}{2l}\sum_{i=0}^{2}\int d\sigma_i\left(\frac{\partial\mathbf{r}_i}{\partial\sigma_i}\right)^2 - f\beta\Delta\sigma_1 - \frac{\beta k(\zeta-\mathbf{X}\chi)^2}{2}}\\ &\quad \delta(\mathbf{r}_1(0)-0)\delta(\mathbf{r}_2(L)-\mathbf{X})\delta(\mathbf{r}_1(\sigma_1+\Delta\sigma_1)-\zeta)\delta(\mathbf{r}_2(\sigma_2+\Delta\sigma_2)-\zeta),\end{aligned} \tag{2.3}$$

where $\beta = \frac{1}{k_BT}$. The Dirac delta function $\delta(\mathbf{r}_1(0)-\mathbf{0})$ imposes the constraint that the fixed crosslink is at the origin while $\delta(\mathbf{r}_2(L)-\mathbf{X}))$ enforces the constraint that the second fixed crosslink is located at an extension $\mathbf{X}$. The crosslinking of the two respective chains by a motor cluster is imposed by the constraint $(\sigma_1+\Delta\sigma_1)-\zeta)\delta(\mathbf{r}_2(\sigma_2+\Delta\sigma_2)-\zeta)$. After performing the functional integrals over $\mathbf{r}_1$ and $\mathbf{r}_2$, the partition function is,

$$\begin{aligned}\mathcal{Z} &= \int_V d^3\zeta\int_{-\sigma_1}^{L-\sigma_1}d\Delta\sigma_1\int d^3\zeta\int_{\mathbf{r}_1(0)=\mathbf{0}}^{\mathbf{r}_1(\sigma_1+\Delta\sigma_1)=\zeta}\mathcal{D}^3\mathbf{r}_1\int_{\mathbf{r}_2(L)=\mathbf{X}}^{\mathbf{r}_1(\sigma_2+\Delta\sigma_1)=\zeta}\mathcal{D}^3\mathbf{r}_2\\ &\quad \exp\left(-\frac{3}{2l}\sum_{i=0}^{2}\int\partial\sigma_1\left(\frac{\partial\mathbf{r}_i}{d\sigma_i}\right)^2 - \mathbf{f}\beta\Delta\sigma_1 - \frac{\beta k(\zeta-\mathbf{X}\chi)^2}{2}\right)\\ &= N\int_{-\sigma_1}^{L-\sigma_1}d\Delta\sigma_1\int_{\zeta=0}^{\zeta=L}d^3\zeta\left(\frac{(2\pi)^2}{((3\ell)^2(\sigma_1+\Delta\sigma_1)(L-\sigma_1-\Delta\sigma_1)}\right)^{\frac{3}{2}}\\ &\quad \exp\left(-\frac{3}{2l}\left(\frac{\zeta^2}{\sigma_1+\Delta\sigma_1}+\frac{(\mathbf{X}-\zeta)^2}{L-\sigma_1-\Delta\sigma_1}\right) - \frac{\beta k(\zeta-\mathbf{X}\chi)^2}{2} - \beta\mathbf{f}\Delta\sigma\right).\end{aligned}$$

To simplify the notation, we denote $S = \sigma_1 + \Delta\sigma_1$ then

$$\begin{aligned}\mathcal{Z} &= \mathcal{N}\exp\left(\beta\mathbf{f}\ell\sigma_1\right)\int_0^L dS\int_V d^3\zeta\left(\frac{(2\pi)^2}{9\ell^2S(L-S)}\right)^{\frac{3}{2}}\\ &\quad \exp\left(-\frac{3}{2l}\left(\frac{\zeta^2}{S}+\frac{(\mathbf{X}-\zeta)^2}{L-S}\right) + \frac{\beta k(\zeta-\mathbf{X}\chi)^2}{2} - \beta\mathbf{f}S\right).\end{aligned} \tag{2.4}$$

For convenience we shall keep the equations in dimensionless units where $S \to Ls$, $\phi \to L\beta f$, $\mathbf{X} \to \ell\mathbf{x}$, and $\ell \to 1$. Absorbing all the constant terms in $\mathcal{N}$ the partition function can be expressed as

$$\mathcal{Z} = \mathcal{N} \int_0^1 ds e^{\frac{3}{2}\ln\left(\frac{1}{R_0^2(3+\beta k R_0^2(1-s)s)}\right) - \frac{3\mathbf{x}^2\left(3+\beta k R_0^2\left(s-2s\chi+\chi^2\right)\right)}{2R_0^2(3+\beta k R_0^2(1-s)s)} - \phi s}, \tag{2.5}$$

where $R_0^2 = \ell L$ denotes the effective spring constant of the polymer chain. In order to get the elastic response of the network on deformation upon varying the fixed crosslinks separation $\mathbf{X}$, first of all, we have to get an analytical expression for the free energy of the network. The free energy is found by taking the logarithm of the partition function.

2.2 Classification of Extension Intervals

The dependence of the exponential term in equation (2.5) on the arc length σ_i and on the extension X is non-trivial. This makes an analytical evaluation of the s integral for the equation not tractable. To perform the calculation, we make use of saddle point approximation method. This amounts to replacing the exponential term in (2.5) by its value at the minimum. In so doing the partition function is approximated by its value at the minimum, which is the point giving the dominant contributions to the free energy of the system. We denote the argument of the exponential in equation (2.5) by

$$g = \frac{3}{2}\ln\left(R_0^2(3+\beta k R_0^2(1-s)s)\right) + \frac{3x^2(3+\beta k R_0^2(s-2s\chi+\chi^2)}{2R_0^2(3+\beta k R_0^2(1-s)s)} + \phi s. \tag{2.6}$$

Solving the saddle point equation

$$\frac{dg(s)}{ds}|_{s^*} = 0 \quad \text{if} \quad \frac{d^2g(s)}{ds^2}|_{s^*} \geqslant 0\,, \tag{2.7}$$

for the critical points. For $\phi = 0$ and $\chi = \frac{1}{2}$ equation (2.7) yields the minima solutions

$$s_1^* = \frac{1}{2} \text{ and } s_{2\pm}^* = \frac{1}{2} \pm \frac{\sqrt{(R_0^2 - x^2)\left(R_0^2 + \frac{12}{k\beta}\right)}}{2R_0^2}. \tag{2.8}$$

Upon exploring different extension limiting cases, we are able to identify specific extension regimes characterised by the location of the minima.

The first critical point $s^* = \frac{1}{2}$ is independent of the network length and spring constant. It is an extremum corresponding to the region of high stretching. It changes from minimum to a local maximum when $x_c = R_0$. The second critical point is a global minimum corresponding to the region of moderate stretching. At lower extensions the minima points for the system drift towards the network end points indicating that, in this regime, the system has a tendency to influence the active crosslink to align towards the strands end points. FIG 2.2 shows a view of g with its extrema for each of the regimes. solving the equation

$$\frac{d^2g(s)}{ds^2}\Big|_{s=s_1^*} = 0, \tag{2.9}$$

we obtain the highest extension, $x_c = R_0$ demarcating the regime of high extension and the regime of moderate extension. This extension is identified as a transition point.

Imposing the condition that $s_2^* = 0$ in (2.8), and solving for x, we obtain the extension $x_0 = 2\left(\frac{3R_0^2}{12+k\beta R_0^2}\right)^{\frac{1}{2}}$ at which the active cross-link reaches the fixed cross-link for the first time as it slides across the strand on deforming the network.

In summary, we refer to the intervals:

- $0 \leq x \leq x_0$ as the regime when the motor has reached the strand endpoints located at the points ($x = 0$ and $x = L$).
- $x_0 \leq x < x_c$ as moderate stretching regime and
- $x > x_c$ as the high stretching regime.

Higher extension, $x > \frac{2L}{3}$, may be explored on account of the infinite extensibility of a Gaussian chain.

2.3 Approximation Scheme and fluctuations

As stated earlier, in order to be able to integrate over the regimes, we approximate g by its value at the minimum where the value of the function gives maximal contribution to the free energy for the system. To incorporate fluctuations about the minima solution, g

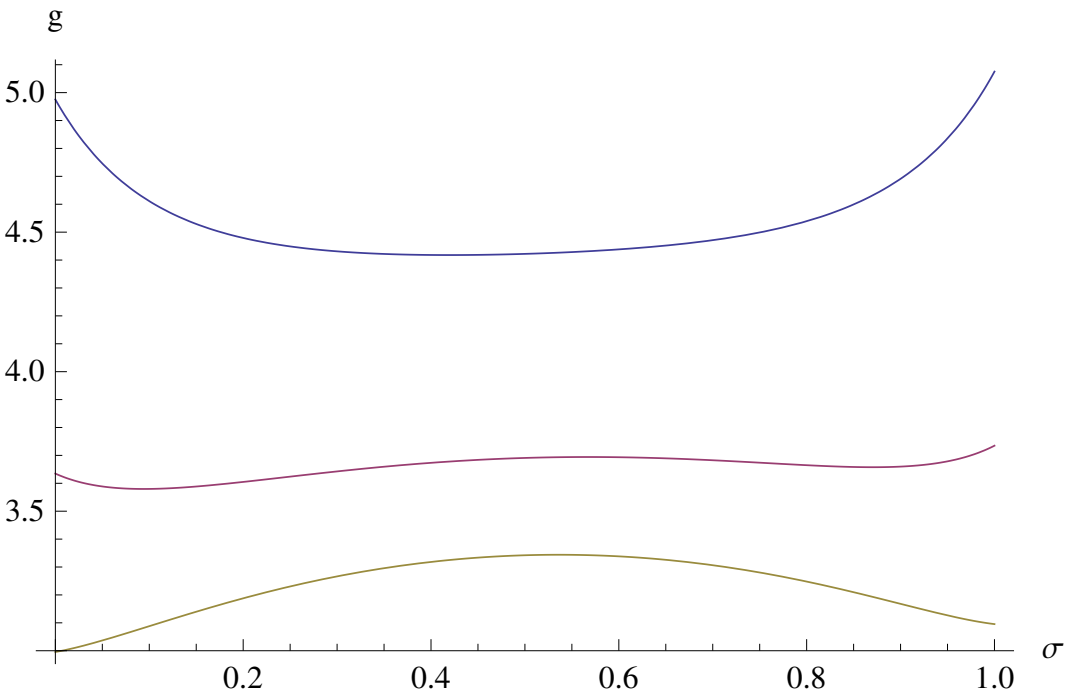

FIG. 2.2. Plots of equation (2.6) for the region of high extension $x = 1.1$ (top curve), moderate stretching regime $x = 0.85$ (middle) and the region where the motor is at the network end points $x = 0.7$ (bottom) for $\{\phi = 0.1, k = 10, R_0 = 1, \beta = 1, \chi = \frac{1}{2}\}$. The graph shows the nature of the minima points for the system for each extension region.

is Taylor expanded around the critical points. This turns out to be a good approximation for the high stretching. The rest of the regimes are sensitive to fluctuations mainly when the curvature goes flat. In this case fluctuations are of the order of the system solution itself. For the case when the molecular motor is at the network end points, it is easy to solve equation (2.5) by numerical integration since the integration is over the arc position s on a finite domain $[0, 1]$.

2.4 Network Elastic Response (No Fluctuations)

For each of the regimes, we work out the expression for tension on the connected strands according to the following set of assumptions:

- We start with the case when there are no fluctuations with a symmetric motor at-

tachment to the background. The tensions for the cases when system has motor force are compared to the tension expression for the cases when there is no motor force.

- Next, we consider the symmetric case ($\chi = \frac{1}{2}$) with fluctuations about the minima solution but with no motor force followed by the scenario where the molecular motors are active. We call these cases "central slipping link".
- Finally, tension expressions for the regimes are calculated for the situation when molecular motors are active with the system having an asymmetric point of attachment. This is a scenario typical of real networks where the other domain is not necessarily connected to the background but connected to another network strand in which case the point of attachment is not necessarily symmetrical.

Under experimental conditions, the case when the motors are inactive $\phi = 0$ is analogous to an instance when the network is submerged in a solution with a very low ATP concentration such that the motors are inactive while the case when $\phi \neq 0$ is analogous to an instance when the network has enough ATP supply such that the motor cluster can generate forces and do work in deforming the connected strands. For $\phi = 0$ we, therefore, refer to the inactive motor as slipping links, since it can translate freely along the chain.

2.4.1 Central Slipping Link Without Force

In the saddle point approximation, the partition function is approximated to

$$\mathcal{Z} = \int_0^1 ds e^{-g(s^*)+\frac{1}{2}(s-s^*)^2\frac{\partial^2 g(s^*)}{\partial s^2}} \approx e^{-g(s^*)}\sqrt{\frac{2\pi}{g''(s^*)}}. \tag{2.10}$$

where fluctuations in g about the minima solution are incorporated through the square root term. When these fluctuations are neglected, with the molecular motors inactive, the partition function for the system is approximated to $\mathcal{Z} = e^{-g(s^*)}$ and the free energy is given by

$$\mathcal{F} = -\frac{1}{\beta}\ln(e^{-g(s^*)}) = \frac{3\left(12+\beta k R_0^2\right)x^2}{8\beta R_0^2\left(3+\beta k R_0^2(1-s^*)s^*\right)} + \frac{3}{2\beta}\ln\left[R_0^2\left(3+\beta k R_0^2(1-s^*)s^*\right)\right] \tag{2.11}$$

For the regime **when the molecular motor cluster reaches fixed crosslinks** $s^* = 0$. i.e lower extension $x \ll x_0$, g becomes

$$g(s^*) = -\frac{x^2\left(12+\beta k R_0^2\right)}{8R_0^2} + \frac{3}{2}\ln\left(\frac{1}{3R_0^2}\right). \tag{2.12}$$

The free energy is therefore given by

$$\beta\mathcal{F} = -\frac{1}{\beta}\ln z = \frac{1}{\beta}\frac{x^2\left(12+\beta k R_0^2\right)}{8R_0^2} + \frac{1}{\beta}\ln(3\sqrt{3R_0^2}). \tag{2.13}$$

Tension on the strand is obtained by taking the derivative of the free energy for the system with respect to the extension x. In this regime tension is found to be

$$T = \frac{1}{\beta}\frac{x\left(12+\beta k R_0^2\right)}{4R_0^2}. \tag{2.14}$$

For the **moderate stretching regime**, the free energy for the system becomes

$$\beta\mathcal{F} = \frac{3}{2}\left(1+\ln\left[\frac{1}{4}x^2\left(12+\beta k R_0^2\right)\right]\right) \tag{2.15}$$

and tension on the connected strand is found to be

$$T = \frac{3}{\beta x}, \tag{2.16}$$

while for the **high stretching regime** the free energy is

$$\beta\mathcal{F} = \frac{3x^2\left(12+\beta k R_0^2\right)}{8R_0^2\left(3+\frac{1}{4}\beta k R_0^2\right)} + \frac{3}{2}\ln\left[R_0^2\left(3+\frac{1}{4}\beta k R_0^2\right)\right] \tag{2.17}$$

and the tension on the strand is

$$T = \frac{3x}{\beta R_0^2}. \tag{2.18}$$

In summary, internal contraction force for the network strand, when fluctuations about the minima solution are neglected is given by

$$T = \begin{cases} \frac{3x}{\beta R_0^2} & x \geq x_c, \\ \frac{3}{\beta x} & x_0 < x < x_c \text{ and} \\ \frac{kx}{4} + \frac{3x}{R_0^2\beta} & 0 \leq x \leq x_0. \end{cases} \tag{2.19}$$

As can it be seen from equation (2.19), when the active crosslink is close to the fixed crosslink $0 \leq x \leq x_0$ and for the high stretching regime $x > x_c$, the force on the strands is analogous to Hooke's law for a spring with effective spring constant given by $\frac{\left(12+kR_0^2\chi^2\right)}{R_0^2\beta}$ and $\frac{3}{\beta R_0^2}$ respectively. Tension for the two regimes is comparable an old result derived in the theory of rubber elasticity which is a basic characteristic of materials, such as rubber, made up of a of chain molecules. The intermediate regime shows a non linear elastic behavior. See FIG 2.3. Looking at the slope of the graphs, we anticipate that there is a possibility of hysteritic behavior for the network tension with extension. The network restoring force increases with temperature hence, reflecting the fact that the force arises from the thermally excited tendency towards disorder.

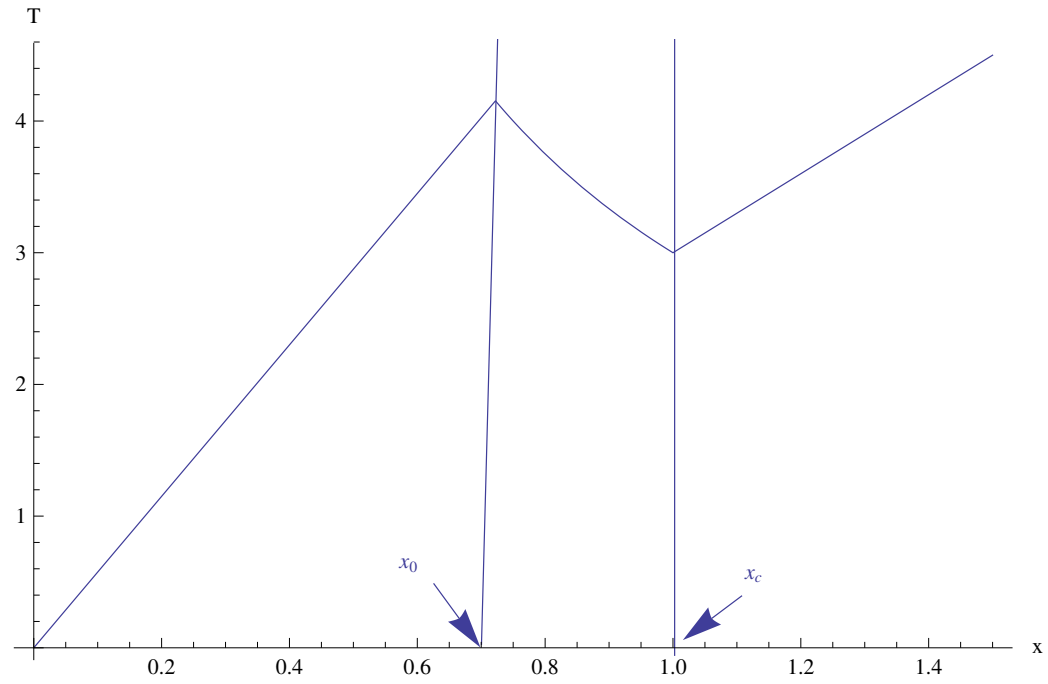

FIG. 2.3. Plot of tension T with extension x for the regime when the active cross link is aligned towards the end of the network strand $0 \leq x \leq x_0$, moderate stretching regime $x_0 < x < x_c$ and High stretching $x > x_c$ regime for $k = 15, \beta = 1, R_0 = 1, \chi = \frac{1}{2}$.

2.5 Network Elastic Response with Fluctuations Included

2.5.1 Central Slipping Link Without Force

In this subsection, fluctuations about the minima solutions are incorporated by taylor series expanding g about the minima solution and the partition functions can be approximated to

$$\mathcal{Z} = \int ds e^{-g(s^*)+\frac{1}{2}(s-s^*)^2\frac{\partial^2 g(s^*)}{\partial s^2}} \approx \left(e^{-g(s^*)}\sqrt{\frac{2\pi}{g^{''}(s^*)}}\right). \tag{2.20}$$

We are interested in exploring how fluctuations affect the elasticity response of the network.

High Stretching Regime

As we have seen in the previous section, solving the steepest descent equations for this regime leads to the minima solutions $s^* = \frac{1}{2}$. At the minima

$$g(s^* = \frac{1}{2}) = \frac{3}{2R_0^2}\left(R_0^2 \ln\left(\frac{4}{\beta k R_0^4 + 12R_0^2}\right) - x^2\right) \quad \text{and} \quad g^{''}(s^* = \frac{1}{2}) = \frac{12\beta k\,(x^2 - R_0^2)}{\beta k R_0^2 + 12}. \tag{2.21}$$

The partition function is found to be

$$\mathcal{Z} \approx \frac{\sqrt{2\pi}4e^{-\frac{3x^2}{2R_0^2}}}{R_0^3\,(12+\beta k R_0^2)\,\sqrt{3\beta k(x^2-R_0^2)}}. \tag{2.22}$$

From equation (2.22), we can see that adding fluctuations around the minimum solution leads to a divergence as x approaches the critical extension x_c . At the critical extension g goes flat and fluctuations dominate the free energy. The Helmholtz free energy of the system is found to be,

$$F = -\frac{1}{\beta}\ln\mathcal{Z} \tag{2.23}$$

$$= \frac{1}{\beta}\ln\left(\frac{4e^{-\frac{3x^2}{2R_0^2}}\sqrt{2\pi}}{R_0^3\,(12+\beta k R_0^2)\,\sqrt{3\beta k(x^2-R_0^2)}}\right) \text{ for } \quad x \neq R_0\ . \tag{2.24}$$

as it was done in the previous section, the internal tension of the network, obtained by taking the derivative of the free energy with respect to extension x is found to be

$$T = \frac{1}{\beta}\left(\frac{2x}{R_0^2} - \frac{x^3}{R_0^2\,(R_0^2 - x^2)}\right) \text{ for } \quad x \neq R_0\ . \tag{2.25}$$

In the above equation, the first term is identical to Hooke's law for a spring. This term dominates for small extension $x < R_0$. The second term dominates as the extension approaches the critical extension leading to a singularity at the critical extension.

Moderate Stretching Regime

For the moderate stretching regime, g has a minima at the critical point s_2^* in equation (2.8). Interestingly enough the minima points in this regime depends on extension. Following a similar line of argument as was done for the high stretching regime, we get

$$g(s_2^*) = \frac{3}{2}\left(\ln\left(\frac{4}{x^2(\beta k R_0^2 + 12)}\right) - 1\right) \quad \text{and} \quad g''(s_2^*) = \frac{24\beta k R_0^4\,(R_0^2 - x^2)}{x^4(\beta k R_0^2 + 12)} \tag{2.26}$$

hence, the partition function can be approximated to,

$$\mathcal{Z} = \frac{4\sqrt{\pi}}{e^{3/2}\,(\beta k R_0^4 x + 12 R_0^2 x)\,\sqrt{3\beta k(R_0^2 - x^2)}} \qquad \text{for } x \neq R_0. \tag{2.27}$$

The free energy is found to be

$$F = \frac{1}{\beta}\ln\left(\frac{4\sqrt{\pi}}{e^{3/2}\,(\beta k R_0^4 x + 12 R_0^2 x)\,\sqrt{3\beta k(R_0^2 - x^2)}}\right) \qquad \text{for } x \neq R_0. \tag{2.28}$$

The force pulling the fixed cross-links together is

$$T = \frac{1}{\beta}\left(\frac{1}{x} - \frac{x}{(R_0^2 - x^2)}\right) \quad \text{for} \quad x \neq R_0. \tag{2.29}$$

In the intermediate regime we witness a non linear force that gets weaker with increasing extension with a trend similar to the tension trend obtained for this regime when fluctuations we excluded. Upon approaching the transition point x_c, fluctuations dominate the system yielding a singularity at $x_c = R_0$.

2.5.2 Central Slipping Link With Force

Under the assumption , $\chi = \frac{1}{2}$ and $\phi = 0$ the free energy of the system is dominated by the entropic contributions of the chain. In this section, we consider the case when $\phi \neq 0$ and we make an assumption that for a small motor force ϕ, the molecular motor cluster at the minimum of g will shift by a small factor ϵ depending on ϕ. When the molecular motor cluster is active

$$g(s,\phi) = \frac{3x^2(\beta k R_0^2 + 12)}{8R_0^2(3 + \beta k R_0^2(s-1)s)} + \frac{3}{2}\log\left(\frac{1}{R_0^2(3 + \beta k R_0^2(s-1)s)}\right) + s\phi. \tag{2.30}$$

For the **high stretching regime** the new minimum $s^* = s_1^* - \epsilon$. Where s_1^* is the critical motor position at zero force. As it was done for the case when there was no motor activity, solving the saddle point equations

$$\begin{aligned}\frac{dg(s,\phi)}{ds}\Big|_{s^*=\frac{1}{2}-\epsilon_1} &= \frac{3x^2(\beta k R_0^2 + 12)\left(\beta k R_0^2\left(\frac{1}{2}-\epsilon_1\right) + \beta k R_0^2\left(-\epsilon_1 - \frac{1}{2}\right)\right)}{8R_0^2\left(\beta k R_0^2\left(-\epsilon_1 - \frac{1}{2}\right)\left(\frac{1}{2}-\epsilon_1\right) - 3\right)^2} \\ &+ \frac{3\left(\beta k R_0^2\left(\frac{1}{2}-\epsilon_1\right) + \beta k R_0^2\left(-\epsilon_1 - \frac{1}{2}\right)\right)}{2\left(\beta k R_0^2\left(-\epsilon_1 - \frac{1}{2}\right)\left(\frac{1}{2}-\epsilon_1\right) - 3\right)} + \phi = 0,\end{aligned} \tag{2.31}$$

leads to the new minima solutions. In order to obtain an explicit equation for the shift ϵ_1, we Taylor series expand equation (2.31) about small ϵ_1 leaving the resulting expression up to first order in ϵ. For small force a shift in the minimum is given by

$$\epsilon_1 = \frac{(12 + k R_0^2\beta)\,\phi}{12k\,(R_0^2 - x^2)\,\beta}. \tag{2.32}$$

The partition function is approximated by $\mathcal{Z} = e^{-g(s_1^* + \epsilon_1)}$ and the free energy

$$\mathcal{F}/k_B T = \frac{1}{2}\left(\frac{3x^2}{R_0^2} + \phi - \frac{(12 + k R_0^2\beta)\,\phi^2}{12k\,(R_0^2 - x^2)\,\beta} + 3\ln\left[3R_0^2 + \frac{1}{4}k R_0^4\beta\right]\right) \tag{2.33}$$

is obtained by taking the logarithm of the partition function. Tension on the strand is found to be

$$T = \frac{1}{\beta}\left(\frac{3x}{R_0^2} - \frac{1}{12}\frac{x\,(12 + k R_0^2\beta)\,\phi^2}{k\,(R_0^2 - x^2)^2\,\beta}\right). \tag{2.34}$$

From the above expression, we see that when the molecular motors are active, in addition to the normal spring-like elastic response, we obtain another term in which molecular

motor force ϕ is couple to the extension x. This suggests that molecular motor activity has an influence on the elasticity of the network in this extension regime. There is no preferential direction on the elastic response with motor force. This is because the motor is symmetrically located. Upon approaching the critical extension, the network tension is sensitive to small motor forces owing to a flat curvature of g. Upon including fluctuations the partition functions is approximated as follows

$$\mathcal{Z} = \int e^{-g(s^*-\epsilon_1,\phi)+\frac{1}{2}(s-(s^*-\epsilon_1))^2\frac{\partial^2 g(s_*-\epsilon_1,\phi)}{\partial s^2}} \approx e^{-g(s_*-\epsilon_1,\phi)}\sqrt{\frac{2\pi}{g''(s_*-\epsilon_1,\phi)}}. \quad (2.35)$$

Using equation (2.32) in equation (2.35) and expanding with respect to a small molecular cluster force ϕ and retaining only up to first order terms in ϕ we obtain the partition function as,

$$\begin{aligned}\mathcal{Z} &= \frac{\sqrt{\frac{\pi}{3}}e^{-\frac{3x^2}{2R_0^2}}\left(-12\beta k\phi\left(R_0^2-x^2\right)^3+24\beta k\left(R_0^2-x^2\right)^3\right)}{6\beta k\left(\beta kR_0^2+12\right)\left(R_0^3-R_0x^2\right)^3\sqrt{\beta k\left(x^2-R_0^2\right)}} \\ &+ \frac{\sqrt{\frac{\pi}{3}}e^{-\frac{3x^2}{2R_0^2}}\left(\phi^2\left(\beta kR_0^6-R_0^4\left(5\beta kx^2+24\right)+8R_0^2x^2\left(\beta kx^2+6\right)-3x^4\left(\beta kx^2+4\right)\right)\right)}{6\beta k\left(\beta kR_0^2+12\right)\left(R_0^3-R_0x^2\right)^3\sqrt{\beta k\left(x^2-R_0^2\right)}}.\end{aligned}$$

The free energy is evaluated by taking the logarithm of the partition function. Taking the derivative of the free energy with respect to the extension, we obtain the analytic expression for tension

$$T = \frac{1}{\beta}\left(\frac{2x}{R_0^2}-\frac{x^3}{R_0^4-R_0^2x^2}+\frac{x\phi^2\left(\beta kR_0^2+12\right)\left(2R_0^4-6R_0^2x^2+x^4\right)}{12\beta k\left(R_0^2-x^2\right)^4}\right). \quad (2.36)$$

From the tension expression above, we realise that in addition to the normal tension obtained without fluctuation we obtain some other terms originating from curvature of g. At the transition extension fluctuations dominate and the expression for tension gets meaningless in this approximation.

Using the same line of argument for the **moderate stretching regime** as for the high stretching regime, a small motor force will shifts the critical point, s_2^*, by a small factor

ϵ depending on the magnitude of the motor cluster force ϕ . The function, $g(s,\phi)$ now become stationary at $s = s^* - \epsilon_2$.

Solving the equation

$$\frac{dg(s,\phi)}{ds}|_{s=s_s^*-\epsilon_2} = \frac{24\beta k R_0^4 \epsilon_2 \left(x^2 - R_0^2\right)}{x^4(\beta k R_0^2 + 12)} - \phi = 0, \tag{2.37}$$

for the shift in the minima ϵ_2, we obtain

$$\epsilon_2 = -\frac{x^4 \left(12 + \beta k R_0^2\right)\phi}{24\beta k R_0^4 \left(R_0^2 - x^2\right)}. \tag{2.38}$$

On incorporating the shift in the minima having ignored fluctuations, the partition $\mathcal{Z} \approx e^{-g(s_2^*+\epsilon_2)}$ and the free energy becomes

$$\begin{aligned}
\mathcal{F}/k_BT &= -\ln(\mathcal{Z}) \\
&= \left(\frac{1}{48}\left(72 + \phi\left(24 - \frac{24\sqrt{kR_0^4(R_0-x)(R_0+x)\beta\left(12+\beta kR_0^2\right)} + \frac{x^4\left(12+\beta kR_0^2\right)\phi}{x^2-R_0^2}}{\beta kR_0^4}\right)\right)\right. \\
&\quad \left. +72\ln\left[\frac{1}{4}x^2\left(12+\beta kR_0^2\right)\right]\right).
\end{aligned} \tag{2.39}$$

Taking the derivative of the free energy with respect to extension x, we obtain tension on the connected strands

$$T = \frac{1}{\beta}\left(\frac{3}{x} + \frac{\left(12x + \beta k R_0^2 x\right)\phi}{2\sqrt{\beta k R_0^4 \left(R_0^2 - x^2\right)\left(12 + \beta k R_0^2\right)}}\right). \tag{2.40}$$

Once again, the motor force ϕ couples with extension x indicating that, small motor force has an influence on tension on the connected strands for the moderate stretching regime. Now considering fluctuations, the partition function with the molecular motors active becomes

$$\mathcal{Z} = \frac{\sqrt{\pi}\left(12\beta k(2-\phi)\left(R_0^3 - R_0x^2\right)^2 - \phi\left(-12R_0^4 + 32R_0^2x^2 - 17x^4\right)\sqrt{\beta k\left(\beta kR_0^2 + 12\right)\left(R_0^2 - x^2\right)}\right)}{6e^{3/2}\beta kx\left(\beta kR_0^2 + 12\right)\left(R_0^3 - R_0x^2\right)^2\sqrt{6\beta kR_0^6 - 6kR_0^4x^2}}. \tag{2.41}$$

Following similar arguments we obtain the network tension for the regime as

$$T = \frac{1}{\beta}\left(\frac{1}{x} - \frac{x}{R_0^2 - x^2} + \frac{x\phi\left(28R_0^4 - 36R_0^2x^2 + 17x^4\right)\sqrt{\beta k R_0^4\left(\beta k R_0^2 + 12\right)\left(R_0^2 - x^2\right)}}{24\beta k R_0^4\left(R_0^2 - x^2\right)^3}\right). \tag{2.42}$$

Once again we uncover the normal tension with some other terms that couple to the motor force ϕ. We learn that there is an increased sensitivity to fluctuations at small motor force as extension approaches x_c.

For the **molecular motor at the network end points**, when the force is switched on, the force does not contribute to the network elasticity and tension on the network strand is given by equation (2.14).

Summary

For the high and moderate stretching regimes, upon activating a small molecular motor force, in addition to the tension term for an inactive network without fluctuations, we get an extra term in which force couples to the extension x in an interesting way. This suggests that molecular motor activity has an influence on the contractility of the network (refer to FIG.2.4). Adding fluctuations, the structure of the tension expressions is preserved. However, at the critical extension, terms originating from curvature renders the saddle point approximation highly inaccurate, because the minimum is very shallow. This is also an aspect that is clearly seen in the numerical comparison as presented in FIG.2.6

A numerical result for tension is obtained by taking the derivative of the partition function (2.5) with respect to extension and numerically integrating the resulting expression over a finite domain. For the plot of the network tension obtained numerically see FIG 2.5. On comparing the tension obtained analytically and the one from numerical integration, we can clearly see that the analytical approach over estimates the elasticity of the network. However, the trends characteristic of each regime feature prominently in both approaches, though very much decreased for the numerical result see FIG 2.6.

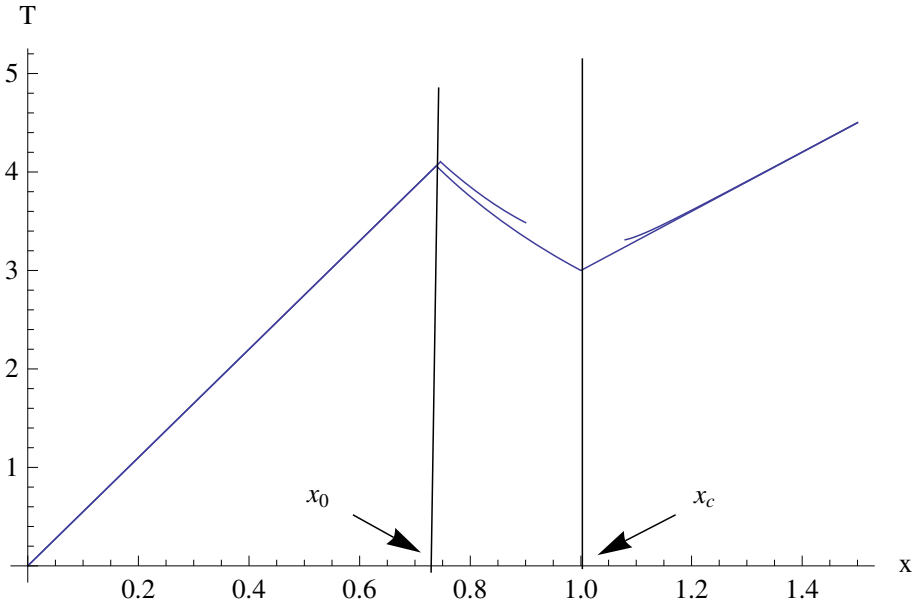

FIG. 2.4. Comparison of the plot tension for the case when there is no motor force equation (2.19), see FIG 2.3, and the case when there is a small motor force $\phi = 0.1$ for the high stretched regime equation (2.34) and moderate stretching regime equation (2.40) and the instance when the motor is aligned towards the fixed crosslink. In each case $\{k = 10, R_0 = 1, \beta = 1, \chi = \frac{1}{2}\}$. We see a shift in tension for the moderate stretching regime and the high stretching regime which suggest the molecular motor force makes the network contract for the two regimes of extension.

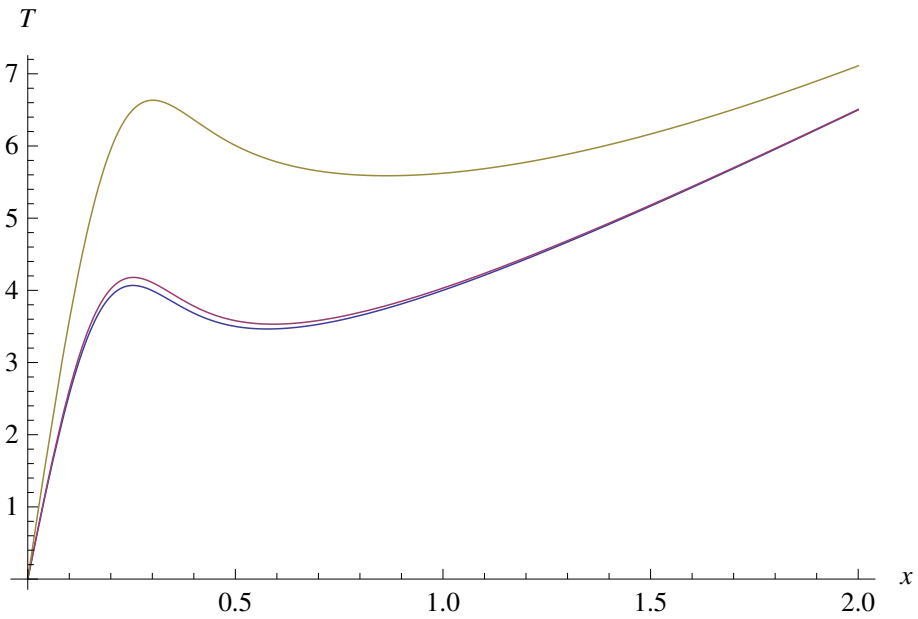

FIG. 2.5. Plot of tension on the network strands for $\phi = 10$ (top graph), $\phi = 1$ (middle graph) and $\phi = 0.1$ (bottom graph) for $\{k = 10, R_0 = 1, \beta = 1, \chi = \frac{1}{2}\}$. This shows that increasing strength of the motor force makes the network more stiffer.

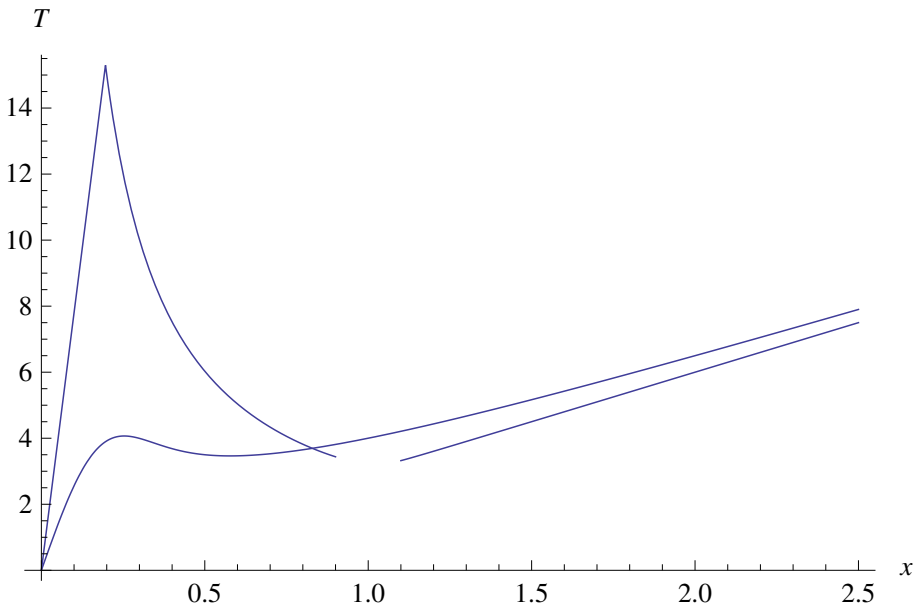

FIG. 2.6. Graph of tension obtain analytically for the all the regimes equations (2.14), (2.34) and (2.40) and graph of tension obtained numerically for $\{\phi = 0.1, k = 150, R_0 = 1, \beta = 1, \chi = \frac{1}{2}\}$. This show that at lower extension, the approximation over estimate the tension. However, for high extension, there is good agreement between the two approaches. At the critical extension $x_c = 1$, the approximation shows a singularity.

2.5.3 Asymmetric Slipping Link With Force

In real networks molecular motor clusters connect one actin strand to another. The resulting network is not necessarily preconditioning the active crosslink to be centrally positioned relative to the fixed crosslinks. As we shall see in section 3.2, the other domain of the motor clusters may be crosslinked to another actin strand which may undergo thermal fluctuations. We anticipate that, as it was the case when introducing activity in the system through a small motor force, the transition extensions x_0 and x_c will also be shifted in response to the asymmetry in the system. Consequently, the free energy and the tension in the network strand will be modified. In this section, we shall introduce a small correction Δ to the symmetry factor χ and show how analytical expressions for the free energy and tension of the system are modified.

Proceeding in a manner analogous to the previous section, we shall start by neglecting fluctuations on approximating the partition function. In this case, the saddle point approximation allows us to write the partition function as $\mathcal{Z} = e^{-g(s_0^*+\epsilon_3,\chi^*+\Delta)}$. Assuming once again that the molecular motor cluster force ϕ is small and that Δ is small, the equation

$$\frac{\partial g(s,\phi)}{\partial s}\Big|_{(s=s^*+\epsilon_3,\chi=\chi^*+\Delta)} = 0 \tag{2.43}$$

can be solved to obtain the correction to the minima

$$\epsilon_3 = \frac{12x^4\phi + kx^4\beta(12\Delta+\phi)R_0^2 - 24kx^2\beta\Delta R_0^4}{24k\beta R_0^4\,(x^2-R_0^2)}. \tag{2.44}$$

The correction, $x^{'}$, to the transition extension x_0 at which the active crosslink reaches the

fixed crosslink for the first time, is obtain by solving the equation

$$\begin{aligned} s_2^* + \epsilon_3 &= \left(\frac{\sqrt{(R_0^2 - x^2)\left(R_0^2 + \frac{12}{k\beta}\right)}}{2R_0^2} + \frac{12x^4\phi + kx^4\beta(12\Delta + \phi)R_0^2 - 24kx^2\beta\Delta R_0^4}{24k\beta R_0^4 (x^2 - R_0^2)} \right)_{|x=x'} \\ &= 0 \end{aligned} \tag{2.45}$$

for $x^{'}$obtaining

$$x_2^{'} = \frac{2\sqrt{3}\left(12\phi + k\beta R_0^2\left(-12\Delta + \phi - 2k\beta\Delta R_0^2\right)\right)}{k\beta R_0\left(12 + k\beta R_0^2\right)^{3/2}}. \tag{2.46}$$

As indicated in the previous section, the free energy is simply

$$\mathcal{F} = k_B T g(s_0^* + \epsilon, \chi^* + \Delta). \tag{2.47}$$

For **the regime when the molecular motor is aligned towards the fixed crosslink**, upon introducing asymmetry through a small factor Δ, free the energy becomes

$$\mathcal{F} = \frac{12x^2 + \left(k\beta(x + 2x\Delta)^2 + 12\mathrm{Log}\left[3R_0^2\right]\right)R_0^2}{8R_0^2} \tag{2.48}$$

and the network tension for the regime is

$$T = \frac{3x}{R_0^2} + \frac{1}{4}kx\beta(1 + 2\Delta)^2. \tag{2.49}$$

As for the **moderate stretching regime** the corrected mimima obtained is

$$s_4^* = s_2^* + \frac{12x^4\phi + kx^4\beta(12\Delta + \phi)R_0^2 - 24kx^2\beta\Delta R_0^4}{24k\beta R_0^4 (x^2 - R_0^2)} \tag{2.50}$$

and the free energy is found to be

$$\begin{aligned} \mathcal{F} &= \frac{1}{2}\left(3 + \phi + 3\ln\left[\frac{1}{4}x^2\left(12 + k\beta R_0^2\right)\right]\right. & (2.51) \\ &+ \left. 12\Delta\sqrt{\frac{k\beta\left(-x^2 + R_0^2\right)}{12 + k\beta R_0^2}} - \frac{\phi\sqrt{k\beta R_0^4\left(-x^2 + R_0^2\right)\left(12 + k\beta R_0^2\right)}}{k\beta R_0^4}\right). & (2.52) \end{aligned}$$

Hence, the tension on the network strands is

$$T = \frac{1}{\beta}\left(\frac{3}{x} + \frac{x\left(12\phi + k\beta(-12\Delta+\phi)R_0^2\right)}{2\sqrt{k\beta R_0^4\left(-x^2+R_0^2\right)\left(12+k\beta R_0^2\right)}}\right). \tag{2.53}$$

Considering the **high stretching regime**, the new minimum is found to be

$$s_3^* = s_1^* + \epsilon_3 = \frac{1}{2} + \frac{12kx^2\beta\Delta - 12\phi - k\beta\phi R_0^2}{12kx^2\beta - 12k\beta R_0^2} \tag{2.54}$$

giving the free energy

$$\begin{aligned}\mathcal{F} &= \frac{3x^2}{2\beta R_0^2} + \frac{1}{2\beta}\left(\phi + 2\left(\ln\left[3R_0^2 + \frac{1}{4}k\beta R_0^4\right]\right)\right.\\ &- \left.\frac{1}{24\beta}\left(\frac{144\phi\left(-2kx^2\beta\Delta+\phi\right) + 24k\beta\left(kx^2\beta\Delta(6\Delta-\phi)+\phi^2\right)R_0^2 + k^2\beta^2\phi^2R_0^4}{k\beta\left(x^2-R_0^2\right)\left(12+k\beta R_0^2\right)}\right)\right).\end{aligned} \tag{2.55}$$

Tension for this regime is given by

$$T = \frac{1}{\beta}\left(\frac{3x}{R_0^2} + \frac{x\left(12\phi + k\beta(-12\Delta+\phi)R_0^2\right)^2}{12k\beta\left(x^2-R_0^2\right)^2\left(12+k\beta R_0^2\right)}\right). \tag{2.56}$$

From the tension expressions (2.49),(2.53) and (2.56) for the respective regimes, obtained by incorporating asymmetry and molecular motor activity, we see that a shift in the symmetry factor Δ couple with extension x indicating that asymmetry has an influence on the network elastic response as well. To see a plot of tension, when there is motor force and asymmetry in the system see FIG 2.7.

2.5.4 Summary

We have learned that the elasticity of a network of a single strands depends on the extension between two fixed cross-links. The behaviour can be characterised into three regimes: the regime when the fixed crosslink is at the wall, the moderate stretching regime and the high extension regime. Tension on the connected strands obeys Hooke's law in the regime when the motor cluster is at the ends and in the high stretching regime. For the moderately stretched regime, the effect of motor activity significantly enhances the internal contractility of the network. We anticipate a hysteretic kind of behaviour on the network tension with extension. Near the transition point $x \approx x_c$ system fluctuations have to be dealt with carefully as they bring about a singularity.

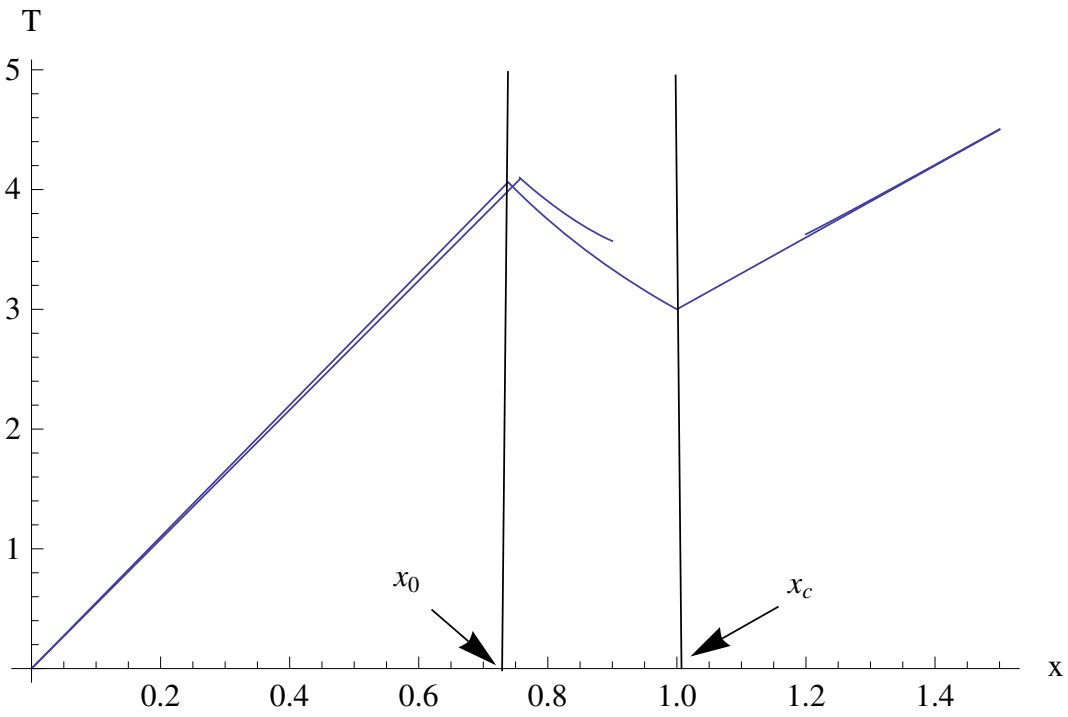

FIG. 2.7. Effect of small correction in the motor attachment symmetry factor $\Delta = 0.1$ on tension for the system with the motors active but with fluctuations ignored for $\{\phi = 0.1, k = 10, R_0 = 1, \beta = 1, \chi = \frac{1}{2}\}$. For the high stretched regime (2.56) and moderate stretching regime (2.53), we see a shift in tension relative to the tension (2.19) for the same system without motor force. This suggest that the presence of activity make the network more resistant to deformation.

Chapter 3

Two Stranded Model With disorder

In the previous chapter, we presented a polymer network model based on the semi-microscopic picture of the entropic elasticity of the chains. The behavior of the model at macroscopic length scale was investigated by deforming the network as an elastic solid by varying the extension $\mathbf{x}$ between fixed crosslinkers. In this chapter we present a theoretical model of a system of (actin) filaments crosslinked at some intermediate position by molecular motor clusters. We connect the semi-microscopic picture and the macroscopic picture by imposing that the network strands are permanently anchored to a non-fluctuating but deformable background that deforms affinely. The background serves a sole purpose of anchoring the network filaments, see FIG. 3.1. The anchoring positions introduce a quenched disorder into the system. A similar construction, but in a different context, has been presented in the works of Rubinstein and Panyukov [28].

We first address a single strand and then expand this to a two strand model. We seek to understand not only the elastic modulus of this system due to motor force but how the activity will make the system contract as well. For these purposes we present results for isovolumetric extension and homogeneous contraction as results for these two extreme cases.

Motivation for the Replica Formalism

So far we have dealt with a system in which the fixed crosslinking position on the chains are known. This is not the case for real networks in biological systems. We can treat these linking positions (quenched degrees of freedom) as variables which differ randomly from one sample of the system to another distributed according to a certain probability. In order to deal with a systems having quenched variables, the standard formulation of statistical mechanics of integrating over all phase space for each particle, as applied to gases, liquids and ordered solids needs modification.

For the current model construction, a permanent anchoring to the background for each realization of the network presents the end-to-end distance as a variable which specifies a disorder in the system. This kind of crosslinking imposes a constraint that the anchoring position should not undergo statistical-mechanical fluctuations but varies with different realizations of the system. The randomness of these linkages between different realizations of the network is the origin of quenched disorder. The theoretical approach we shall employ here originates from the pioneering contribution to the theory of condensed matter: The Deam-Edwards [6] theory of single crosslinked macromolecules and the Edwards-Anderson theory of spin glass [10]. This method take care of these quenched random variables statistically as well and it accounts for their quenched nature by invoking the replica technique.

Considering a particular copy of the network, the final free energy of system F_c would be given by the logarithm of the partition function

$$e^{-\beta F_c} = \mathcal{Z}_c = \int e^{-\beta H} d\Omega_c. \tag{3.1}$$

where H is the hamiltonian and $\int d\Omega_c$ is integration over all the available conformations when the motors are switched on. The label c, for a specific sample, restricts the conformations to the crosslinked topology with a particular set of quenched variables $c = \{\mathbf{R}_i\}$.

As Deam and Edwards [6] argued, a crosslinked chain is constrained to have a mean position in the network owing to the crosslinks. This means that the positions will transform in an affine manner, $\mathbf{R} \to \mathbf{\Lambda R}$ on deforming the network. In our case, $\mathbf{\Lambda}$ is a 3×3 tensor of the

form [1]

$$\mathbf{\Lambda} = \begin{pmatrix} \lambda_1 & 0 & 0 \\ 0 & \lambda_2 & 0 \\ 0 & 0 & \lambda_3 \end{pmatrix} \qquad \lambda_i > 0 \text{ for } i \in \{1, 2, 3\}. \tag{3.2}$$

where λ_i is the extension ratio defined as the deformed length in the direction i divided by the original network length. When the network copy is deformed, the free energy would be given by the logarithm of

$$e^{-\beta F_c(\Lambda)} = \tilde{\mathcal{Z}}_c = \int e^{-\beta H} d\tilde{\Omega}_c. \tag{3.3}$$

The correct experimental free energy of the network, is obtained by averaging the final free energy $F_c(\Lambda)$ with respect to the probability distribution P_c which, for the subsequent calculation, shall assumed to be the probability distribution for the network strands end points being anchored at a particular set $\{\mathbf{R}_i\}$. For the second model calculation P_c shall be assumed to be the network formation probability or probability of an undeformed copy of the system, which is perceived to be the probability at the most relaxed network conformation[2]. This shall be incorporated through the replica trick as the zeroth replica. The disorder averaged free energy is given by:

$$\mathcal{F} = -k_B T \int P_c(\mathbf{R}_i) F_c(\{\mathbf{\Lambda R}_i\}) \prod_i d\mathbf{R}_i = -k_B T \int P_c(\mathbf{R}_i) \ln \mathcal{Z}(\{\mathbf{\Lambda R}_i\}) \prod_i d\mathbf{R}_i \tag{3.4}$$

On averaging over the logarithm with respect to the disorder, in the above equation, the replica trick allows us to introduce a very large number of copies of the system with disorder in the crosslinking topology. In so doing we pay the price by introducing a strange and rather complicated effective coupling amongst the replicated monomer degrees of freedom. The application of the replica trick help us to do away with the quenched random variables.

[1] Owing to its experimental simplicity [29], we shall be mostly interested in isovolumetric uniaxial deformation, where a stretching (compression) by a factor λ_1 along the x axis leads to a compression (enlogation) by a factor $\frac{1}{\sqrt{\lambda_1}}$ along the other axis. This deformation will change the gel shape without affecting its volume. Pure homogeneous deformations of incompressible gels solutions could be coved by bi-axial strain where $\lambda_1 = \lambda_2 = \lambda_3$.

[2] This approach for dealing with disorder works because the network formation probability P_c is assumed to be known in advance as it can be established at fabrication and it does not change on deforming the system [6].

At the end we obtain what can be called, in statistical mechanics sense, a weighted averaged free energy of the deformed and undeformed system. This is an extensive quantity, i.e. it correspond to an experimentally measurable free energy.

For the model under consideration, the introduction of replicas turns out to be a practical approach, as mathematically, we can specify the network topology and keep it conserved, over deformation, by imposing crosslinking constraints.

3.1 Reduced single Strand Model With a Tether

To model the system, we assume that there are n_c randomly distributed phantom chains of effective length L. The far ends of the chains are crosslinked to the background while at some intermediate positions $\boldsymbol{\zeta_i}$, the chains are crosslinked to a molecular motor cluster. The molecular motors clusters are such that their binding head is attached to the background while the other active head is connected to the chains. As in the previous chapter, the actin strand is thought of as consisting of two subchains of length L_1 and L_2 that are crosslinked at the location of active motor cluster domain. The two subchains are parameterised by position vectors $\mathbf{r}_i(s_i) \quad \text{for} \quad i \in \{1, 2\}$, where s_1 and $s_2 \in [0, L]$. For a schematic view of the model construction see FIG. 3.1.

With respect to our basic ingredients, we continue with the approach introduced in the previous chapter where the detailed microscopic description of actin monomers and molecular motor clusters' chemistry features only in the extent that they determine the following parameters: the total arc-length of each actin filament, persistence length, spring constant and the motor force. As it was the case in the first chapter, we think of the network strands as flexible linear objects, that are capable of exhibiting a large number of configurations and we employ classical statistical mechanics to describe the properties of a system composed of thermodynamically large number of this kind of crosslinked actin filaments.

We denote the statistical partition function for the crosslinked system by

$$\mathcal{Z}(\{\mathbf{R}, \chi\}) \quad = \quad \left\langle \Pi_{j=1}^{n_c} \delta(\mathbf{r}_1(s_{1j}) - \mathbf{r}_2(s_{2j})) \right\rangle_E , \tag{3.5}$$

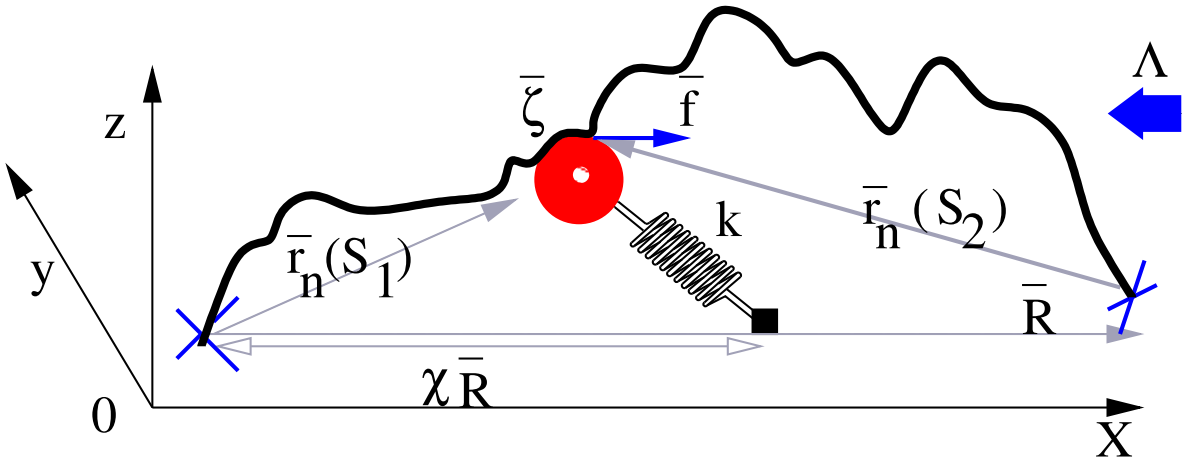

FIG. 3.1. The network consist of a single actin strand whose ends are crosslinked to the background, separated by a distance $\mathbf{R}$ apart. The strand is crosslinked to a molecular motor cluster active head (red) at $\boldsymbol{\zeta}$. The other head of the motor cluster is crosslinked to the background at $\chi\mathbf{R}$. The tether connecting the motor active heads is modelled as a spring of stiffness k. As in the previous model construction see FIG. 2.1 the binding heads of the motor translate along the strand effecting a biasing force f. The network is subject to an external deformation represented by a deformation tensor Λ.

where $\mathbf{R}$ is the end-to-end distance of the chain, χ determines where between the fixed crosslinks the other active motor cluster is anchored. The product of the delta function serves to enforce the crosslinking constraint $\mathbf{r}_1 = \mathbf{r}_2$ for each of the networks. The subscript E serve to remind us that the weight of the remaining contributions is given by the Edwards measure. The partition function is stated as follows

$$\mathcal{Z} = \int_0^{L_1} ds_1^\alpha \int_0^{L_2} ds_2^\alpha \int_v d\boldsymbol{\zeta} \int_{\mathbf{r}_1^\alpha(0)=0}^{\mathbf{r}_1^\alpha(s_1)=\boldsymbol{\zeta}^\alpha} \mathcal{D}\mathbf{r}_1^\alpha \int_{\mathbf{r}_2^\alpha(s_2)=\boldsymbol{\zeta}^\alpha}^{\mathbf{r}_2^\alpha(0)=\boldsymbol{\Lambda}\mathbf{R}} \mathcal{D}\mathbf{r}_2^\alpha \quad e^{-\beta H^\alpha}. \tag{3.6}$$

The superscript α anticipates the introduction of replicas to the system. The Edwards measure for the system is constituted by the hamiltonian

$$\beta H(\{s_i^\alpha\}_{i=1}^2, \boldsymbol{\zeta}^\alpha, \chi, \mathbf{f}, \boldsymbol{\Lambda}\mathbf{R}) = -\frac{3}{2l}\sum_{i=1}^{2}\int_0^{L_i} ds_i^\alpha \left(\frac{\partial \mathbf{r}_i^\alpha}{\partial s_i^\alpha}\right)^2 - \frac{\beta k}{2}(\boldsymbol{\zeta}^\alpha - \chi\Lambda\mathbf{R})^2 + \beta f L \Delta s_i^\alpha. \tag{3.7}$$

where the full length of the network strand $L = L_1 + L_2$. This hamiltonian is similar to that in the previous model calculation, equation (2.2), except for the replica index in the non quenched variables. The free energy of the system for a particular anchoring state

$\{\chi, \mathbf{R}\}$ is given by

$$F(\{\chi, \mathbf{\Lambda R}\}) = -k_B T \ln \mathcal{Z}(\{\chi, \mathbf{\Lambda R}\}), \tag{3.8}$$

We assume a Gaussian distribution, $P(\mathbf{R})$, of the end to end distance $\mathbf{R}$. Then for a canonical ensemble of n_c networks of this kind of crosslinking topology, the disorder averaged free energy is given by

$$\begin{aligned} \mathcal{F} &= [F(\chi, \mathbf{R})]_d \\ &= \frac{-k_B T}{n_c} \sum_{i=1}^{n_c} \int_0^1 d\chi_i \int_v d\mathbf{R} P(\mathbf{R}) \ln \mathcal{Z}(\chi, \Lambda \mathbf{R}). \end{aligned} \tag{3.9}$$

Where $[\cdots]_d$ denotes an average with respect to the disorder. Because all the chains of the system are equivalent the summation can be replaced by the number of networks n_c leading to

$$\begin{aligned} \mathcal{F} &= -k_B T \int_0^1 d\chi \int_v d\mathbf{R} e^{-\frac{3\mathbf{R}^2}{2R_0^2}} \ln \left[\int_0^{L_1} ds_1^\alpha \int_0^{L_2} ds_2^\alpha \int_v d^3\boldsymbol{\zeta}^\alpha \int_v d^3\mathbf{r}^\alpha e^{-\beta H(\{s_i^\alpha\}_{i=1}^2, \boldsymbol{\zeta}^\alpha, \{\mathbf{r}^\alpha\}_{i=1}^2, \chi,)} \right] \\ &= -k_B T \int_0^1 d\chi \int_v d\mathbf{R} e^{-\frac{3\mathbf{R}^2}{2R_0^2}} \left\{ \ln \left[\int_0^{L_1} ds_1^\alpha \int_0^{L_2} ds_2^\alpha \int_v d^3\boldsymbol{\zeta}^\alpha \left(\frac{(2\pi)^2}{\ell^2 (s_1^\alpha) s_2^\alpha} \right)^{\frac{3}{2}} \right. \right. \\ &\quad \left. \left. \exp\left(-\frac{3}{2R_0^2} \left(\frac{\boldsymbol{\zeta}^{\alpha 2}}{s_1^\alpha} + \frac{(\mathbf{\Lambda R} - \boldsymbol{\zeta}^\alpha)^2}{s_2^\alpha} - \right) - \frac{\beta k (\boldsymbol{\zeta}^\alpha - \chi \mathbf{\Lambda R})^2}{2} + \beta L f s_1^\alpha \right) \right] - 1 \right\}, \end{aligned} \tag{3.10}$$

where we have performed the functional integral over $\mathbf{r_1}$ and $\mathbf{r}_2$. Recalling that the length of the full strand $L = L_1 + L_2$, expressed in terms of s_1^α the arc coordinate $s_2^\alpha = L - s_1^\alpha$. In dimensionless units $s_1^\alpha \to L s^\alpha$. The effective free energy can therefore be written as

$$\begin{aligned} \mathcal{F} &= -k_B T \int_0^1 d\chi \int_v d\mathbf{R} e^{-\frac{3\mathbf{R}^2}{2R_0^2}} \left\{ \ln \left[\int_0^1 ds^\alpha \int_v d^3\boldsymbol{\zeta}^\alpha \left(\frac{(2\pi)^2}{R_0^4 (1 - s^\alpha) s^\alpha} \right)^{\frac{3}{2}} \right. \right. \\ &\quad \left. \left. \exp\left(-\frac{3}{2R_0^2} \left(\frac{\boldsymbol{\zeta}^{\alpha 2}}{s^\alpha} + \frac{(\mathbf{\Lambda R} - \boldsymbol{\zeta}^\alpha)^2}{1 - s^\alpha} - \right) - \frac{\beta k (\boldsymbol{\zeta}^\alpha - \chi \mathbf{\Lambda R})^2}{2} + \beta L f s^\alpha \right) \right] - 1 \right\}. \end{aligned} \tag{3.11}$$

The average in equation (3.11) is generally difficult to compute mainly because of the dependence of the partition function on s^α. In order to perform the average, the following

identity is used:

$$\lim_{n\to 0}\frac{\mathcal{Z}^n-1}{n}=\ln\mathcal{Z}\quad\text{or}\quad\frac{\partial\mathcal{Z}^n}{\partial n}|_{n=0}=\ln\mathcal{Z}, \tag{3.12}$$

which is in resemblance to an annealed average. This forms the core of the *replica technique*. Rather than writing $\mathcal{Z}^n(\{s^\alpha,\boldsymbol{\zeta}_i\})=\int d^n\boldsymbol{\zeta}_i d^n s e^{-nH(\{\boldsymbol{\zeta}_i\})}$, this can be conveniently expressed as a system of replicas and instead we can use:

$$\mathcal{Z}^n(\{s^\alpha,\boldsymbol{\zeta}_i^\alpha\})=\int\prod_{\alpha=1}^{n}d\boldsymbol{\zeta}_i^\alpha\prod_{\alpha=1}^{n}ds^\alpha e^{\sum_\alpha H(\{s^\alpha,\boldsymbol{\zeta}_i^\alpha\})}, \tag{3.13}$$

where all variables which are not exhibiting disorder for the system are labelled with the superscript $\alpha\in 1,2,\cdots n$. Essentially, in so doing, the system is duplicated n times with each system having the similar anchoring topology which stays fixed for a particular copy of the system but which can vary between different realizations of the system. The chains are allowed to undergo arbitrary thermal fluctuations for each copy.

3.1.1 Details of replica calculation

After performing the integration over the intermediate positions $\boldsymbol{\zeta}^\alpha$, we can use the identity in (3.12), and the logarithm term can be replaced by the following expression:

$$\begin{aligned}&\int_0^1\prod_{\alpha=1}^{n}ds^\alpha\left(\frac{1}{(3+\beta kR_0^2(1-s^\alpha)s^\alpha)}\right)^{\frac{3}{2}}\\&\exp\left\{-\frac{(3\Lambda\mathbf{R})_0^2}{2R_0^2}\sum_{\alpha=1}^{n}\left(1+\frac{(3+\beta kR_0^2\left(s^\alpha-2s^\alpha\chi+\chi^2\right))}{\left(3+k\beta R_0^2\left(1-s^\alpha\right)s^\alpha\right)}\right)\right.\\&\left.+\sum_{\alpha=0}^{n}\beta fLs^\alpha\right\}.\end{aligned}$$

The advantage of having used the replica technique is that all the disorder variables could be dealt with before the s integral. Performing the Gaussian integral in $\mathbf{R}$ yields ,

$$
\begin{aligned}
[\mathcal{Z}^n]_d &= \int_0^1 d\chi \frac{1}{n}\left[\int_0^1 \prod_{\alpha=1}^{n} ds^\alpha \left(\frac{\exp(\frac{2f\beta L s^\alpha}{3})}{3+\beta k R_0^2(1-s^\alpha)s^\alpha}\right)^{\frac{3n}{2}}\right. \\
&\quad \left.\left\{\prod_{\imath=1}^{3} \frac{1}{\sqrt{1+\lambda_i^2\sum_{\alpha=1}^{n}\left\{\frac{\left(3+\beta k R_0^2\beta(s^\alpha-2s^\alpha\chi+\chi^2)\right)}{\left(3+\beta k R_0^2(1-s^\alpha)s^\alpha\right)}\right\}}}\right\}\right] \\
&= \int_0^1 d\chi I_0^n \left\langle \prod_{\imath=1}^{3}\left(1+\lambda_i^2\sum_{\alpha=1}^{n}\left\{\frac{\left(3+\beta k R_0^2\left(s^\alpha-2s^\alpha\chi+\chi^2\right)\right)}{\left(3+\beta k R_0^2\left(1-s^\alpha\right)s^\alpha\right)}\right\}\right)^{-\frac{1}{2}}\right\rangle_0 \qquad (3.14)
\end{aligned}
$$

where

$$
I_0 = \int_0^1 ds^\alpha \left(\frac{1}{\left(3+\beta k R_0^2\left(1-s^\alpha\right)s^\alpha\right)}\right)^{3/2} e^{(-\beta f L s^\alpha)}. \qquad (3.15)
$$

We define the average $\langle\cdots\rangle_0$ as

$$
\langle\cdots\rangle_0 = \frac{\int_0^1 ds^\alpha(\cdots)\left(\frac{1}{\left(3+\beta k R_0^2(1-s^\alpha)s^\alpha\right)}\right)^{3/2} e^{(-\beta f L s^\alpha)}}{\int_0^1 ds^\alpha \left(\frac{1}{\left(3+\beta k R_0^2(1-s^\alpha)s^\alpha\right)}\right)^{3/2} e^{(-\beta f L s^\alpha)}}. \qquad (3.16)
$$

in equation (3.14). Denoting $Y^\alpha = \lambda_i^2\left\{\frac{\left(3+\beta k R_0^2\left(s^\alpha-2s^\alpha\chi+\chi^2\right)\right)}{\left(3+\beta k R_0^2(1-s^\alpha)s^\alpha\right)}\right\}$, we can approximate

$$
\left\langle \frac{1}{\sqrt{1+\sum_{\alpha=1}^{n} Y^\alpha}}\right\rangle_0 \approx \frac{1}{\sqrt{1+\sum_{\alpha=1}^{n}\langle Y^\alpha\rangle_0}} \approx 1-\frac{1}{2}\sum_{\alpha}^{n}\langle Y^\alpha\rangle_0 + O(n^2). \qquad (3.17)
$$

Because at the end we have to take the replica limit, shown in equation (3.12), we are only interested in terms up to first order in the replica index n. Assuming that the replicas are symmetric

$$
\sum_{\alpha=0}^{n}\left\{\frac{\left(3+\beta k R_0^2\left(s^\alpha-2s^\alpha\chi+\chi^2\right)\right)}{2\left(3+\beta k R_0^2\left(1-s^\alpha\right)s^\alpha\right)}\right\} \to n\left\{\frac{\left(3+\beta k R_0^2\beta\left(s^\alpha-2s^\alpha\chi+\chi^2\right)\right)}{2\left(3+\beta k R_0^2\left(1-s^\alpha\right)s^\alpha\right)}\right\}. \qquad (3.18)
$$

To first order in n, $I_0^n = e^{n \ln I_0} \approx 1 + n \ln I_0$. Since the tether connecting the active motor cluster heads is assumed to weakly couple the active domains, the resulting expressions expanded in a Taylor series about small k leads to

$$\begin{aligned}[\mathcal{Z}^n]_d &= 1 - \frac{n}{2\widetilde{I}_0} \int_0^1 d\chi \int_0^1 ds \sum_i^3 \lambda_i^2 \frac{(6 + kR_0^2\beta\,(5s^2 + 2\chi^2 - s(3+4\chi)))}{18\sqrt{3}} \exp(-\beta L f s) \\ &+ \frac{n}{\widetilde{I}_0} \ln\left[\widetilde{I}_0\right] \end{aligned} \tag{3.19}$$

Here $\widetilde{I}_0 = \int_0^1 ds \frac{2+k\beta R_0^2 s(s-1)}{6\sqrt{3}} \exp\left(-\beta L f s\right)$ is obtained by expressing I_0 up to first order in the molecular motor tether spring constant k. Now performing the χ integral, we obtain,

$$\begin{aligned}[\mathcal{Z}^n]_d &= 1 - \frac{n}{2\widetilde{I}_0} \int_0^1 ds \sum_i^3 \lambda_i^2 \left(\frac{\left(18 + \beta \mathrm{kR}_0^2\,(2 - 15s + 15s^2)\right)}{54\sqrt{3}} \right) \exp(-\beta L f s) \\ &+ \frac{n}{\widetilde{I}_0} \ln\left[\widetilde{I}_0\right]. \end{aligned} \tag{3.20}$$

Assuming small motor force f, the remaining integrals could be performed with ease leading to an expression for the disorder averaged partition which function depends on the polymer chain spring constant R_0^2, spring constant of the tether k and the motor force f.

$$\begin{aligned}[\mathcal{Z}^n]_d &= 1 - n \sum_{i=1}^3 \lambda_i^2 \left(\frac{(36 - k\beta R_0^2)}{2\,(12 - k\beta R_0^2)} - \frac{(72 - k\beta R_0^2)\,(\beta f L)^2}{36\,(12 - k\beta R_0^2)} \right) \\ &+ \frac{n}{\left(\frac{(\beta L f + 2)(12 - \beta k R_0^2)}{72\sqrt{3}}\right)} \ln\left[\left(\frac{(\beta L f) + 2)(12 - \beta k R_0^2)}{72\sqrt{3}} \right) \right] \end{aligned} \tag{3.21}$$

For a weak tether, the disorder averaged partition function can be approximated to

$$\begin{aligned}[\mathcal{Z}^n]_d &\approx 1 - n \sum_{i=1}^3 \lambda_i^2 \frac{1}{36} \left(18 + \beta k R_0^2\right) - n \sum_{i=1}^3 \lambda_i^2 \frac{1}{432} \left(72 + 5k\beta R_0^2\right) (\beta f L)^2 \\ &- \frac{n}{16}\sqrt{3}(12(6\ln(3) - \beta L f(2 + \ln(27))) + k\beta R_0^2(4 + 6\ln(3) \\ &- \beta L f(4 + \ln(27)))) \end{aligned} \tag{3.22}$$

Upon substituting this into equation (3.12), and taking the replica limit, we finally get the

effective free energy as

$$\begin{aligned}\frac{\mathcal{F}}{k_BT} &= \sum_{i=1}^{3}\lambda_i^2\frac{1}{36}\left(18+\beta k R_0^2\right)+n\sum_{i=1}^{3}\lambda_i^2\frac{1}{432}\left(72+5k\beta R_0^2\right)(\beta f L)^2 \\ &+ \frac{n}{16}\sqrt{3}\left(12(6\ln(3)-\beta L f\,(2+\ln(27)))+k\beta R_0^2(4+6\ln(3)\right. \\ &- \left.\beta L f(4+\ln(27)))\right). \end{aligned} \tag{3.23}$$

If the network is enclosed within an ATP solution of constant volume V, the network has a tendency to shrink. The internal contraction force T is balanced by the opposing hydrostatic force P equal in all directions. For an incompressible solution, assuming that the network is stretched by a factor λ_1 in the x direction, the constant volume condition demands that the network dimensions in the y and z directions are reduced by a factor $\frac{1}{\sqrt{\lambda_1}}$ therefore, the free energy becomes

$$\begin{aligned}\frac{\mathcal{F}}{k_BT} &= \left(\lambda_1-\frac{1}{\lambda_1^2}\right)\left(\frac{1}{18}\left(18+\beta^2 k R_0^2\right)+\frac{1}{432}\left(72+5k\beta R_0^2\right)(\beta f L)^2\right) \\ &+ \frac{n}{16}\sqrt{3}(12(6\ln(3)-\beta L f(2+\ln(27)))+k\beta R_0^2(4+6\ln(3) \\ &- \beta L f(4+\ln(27)))). \end{aligned} \tag{3.24}$$

3.1.2 Elasticity results

The contraction force of the chains in the x direction,

$$T_x = k_BT\left(\lambda_1-\frac{1}{\lambda_1^2}\right)\left(\frac{1}{18}\left(18+\beta k R_0^2\right)+\frac{1}{432}\left(72+5k\beta R_0^2\right)(\beta f L)^2\right), \tag{3.25}$$

is obtained by taking the derivative of the free energy with respect to λ_1.

In equation (3.24) the factor $\left(\lambda_1-\frac{1}{\lambda_1^2}\right)$ is typical of classical theory of rubber elasticity [13]. The deformation factor is modified by a term which depends on the ratio of the natural spring constant of the chain R_0^2 and the temperature dependent spring constant of the molecular motor βk together with a term which depends on the molecular motor force $(f\beta L)^2$. Two limiting cases could be discussed. First if the molecular motors are not active, $f = 0$ for instance, the tension reduces to the tension of a normal network modified

by the ratio $\beta k R_0^2$. If the ratio $\beta k R_0^2$ is very small, the tension degenerate to the normal elastic response modified the motor force. This is because we still have the slipping link.

Under uniaxial isovolumetric stretching, $V = (X\lambda_1)^3$, where X has the dimension of length. The variation in the pressure that balances the above tension is given by

$$\begin{aligned} \mathcal{P} &= = -\frac{\partial V}{\partial \lambda_1}\frac{\partial \mathcal{F}}{\partial V} \\ &= -k_B T \frac{2}{9X^6}\left(\frac{1}{\lambda_1^3} - \frac{1}{\lambda_1^6}\right)\left(\frac{1}{18}\left(18 + \beta k R_0^2\right) + \frac{1}{432}\left(72 + 5k\beta R_0^2\right)(\beta f L)^2\right) \end{aligned} \quad (3.26)$$

The pressure is also subject to the above discussed limiting cases and it goes through a maximum at $\lambda_1 = \frac{1}{\sqrt{3}}$.

3.2 Two Strand Model

In this section, we present a calculation for the partition function for a network of two chains crosslinked to each other by a molecular motor cluster see FIG 3.2 . In this context, the molecular motors crosslinks are still assumed to be of slipping link nature. They constrain certain randomly chosen actin strands to remain adjacent to one another while the far ends of the filaments remain crosslinked to the background. Once again, we shall resort to the replica technique to average over the disorder but in a slightly different formulation. In the previous section we showed that the effective energy of elasticity $\mathcal{F}(\mathbf{\Lambda})$ can be obtained by taking a quenched average of the sample free energy $F_c(\{\mathbf{\Lambda R}_i\}_{i=1}^2)$ over all possible realization of the arclength locations $C = \{\mathbf{R}_i\}_{i=1}^2$. with

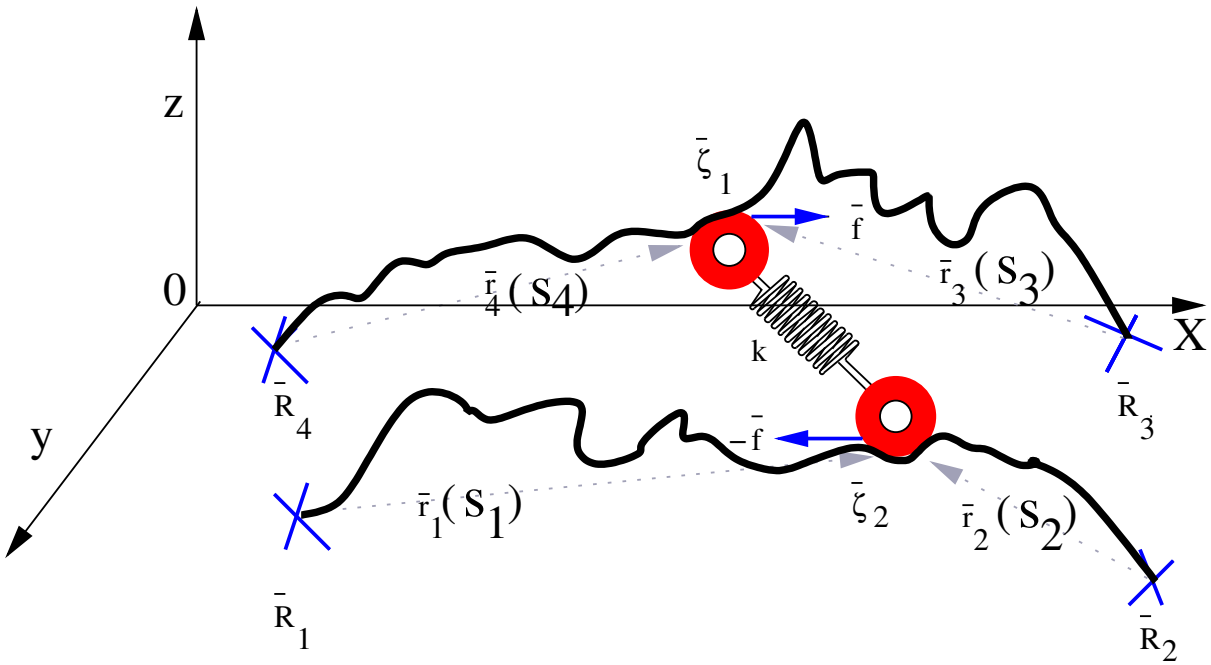

FIG. 3.2. The figure shows a network consisting of two actin strands crosslinked by a progressive molecular motor cluster (shown in red) at some intermediate position ζ_1 and ζ_2 along the respective strands. The network end points are anchored to a non fluctuating background at positions $\{\mathbf{R}_1, \mathbf{R}_2, \mathbf{R}_3, \mathbf{R}_4\}$. The molecular motors exert a directionally reversible force along the strands. The tether connecting the two active motor cluster domains is modelled as a spring of strength k.

$$\mathcal{F}(\Lambda) = \int P(\{\mathbf{R}_i\})_c F(\{\mathbf{\Lambda R}_i\}) \prod_i d\mathbf{R}_i = \int P(\{\mathbf{R}_i\})_c \ln \mathcal{Z}(\{\mathbf{\Lambda R}_i\}) \prod_i d\mathbf{R}_i. \qquad (3.27)$$

It is possible to include the probability P_c as the zeroth replica $\mathcal{Z}^{(0)}$. In this sense, P_c is the probability of a copy of the system that is crosslinked by the molecular motor cluster prior to the activation of the motor force. This is an undeformed copy of the system at a most relaxed polymer conformation. Thus there are $n+1$ copies of the system, see FIG.3.3.

For the two strand model under consideration the propagator or greens function representation for the four segments attached to the motor heads with the degrees of freedom frozen at $\{\mathbf{R}_i\}_{i=1}^4$ could be expressed as a product of separable paths

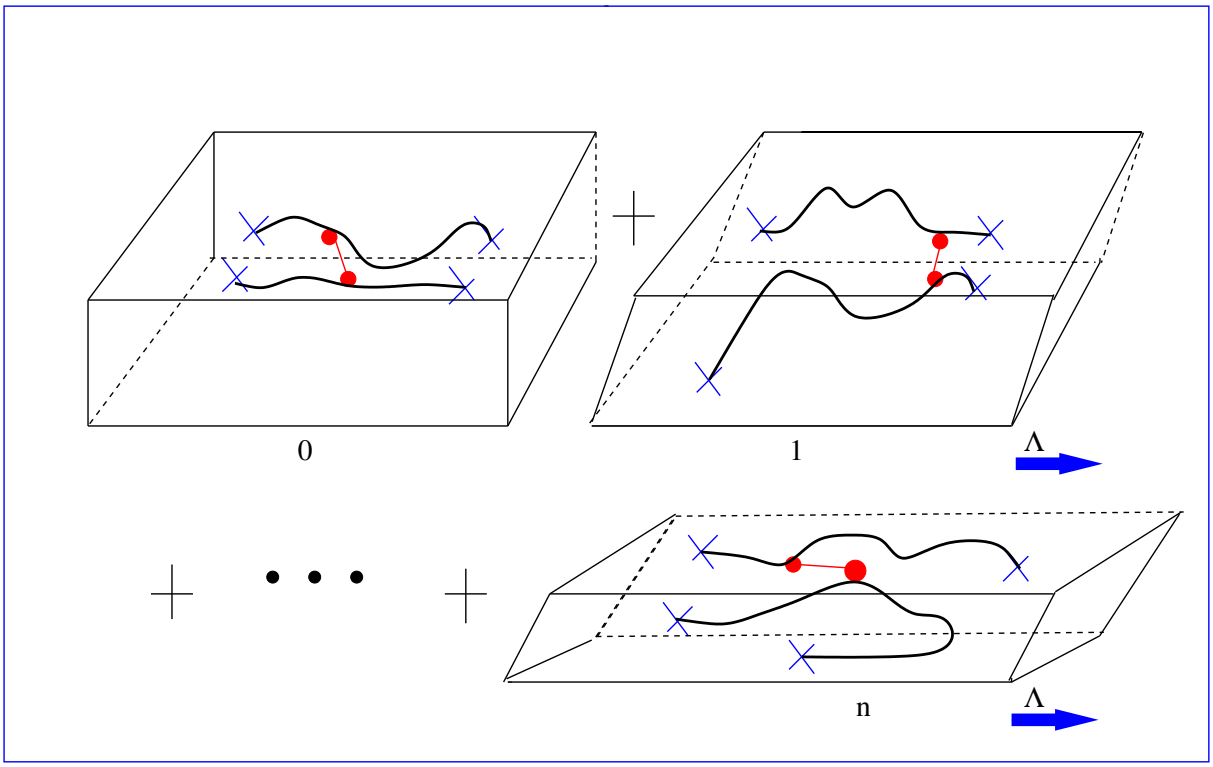

FIG. 3.3. This figure shows a system of $n+1$ network replicas of the type show in FIG.3.2 , the zeroth replica is the network at the most relaxed polymer conformation, i.e before the molecular motors are active. The other replicas (high replica sector) are the copy of the zeroth replica which may be differently deformed either through mechanical strain at a constant volume or which may be at a different temperature. The molecular motors in the high replica sector are presumed to be fully active.

$$\mathcal{Z}(\{\mathbf{R}_i\}_{i=1}^4, \boldsymbol{\zeta_1}, \boldsymbol{\zeta_2}) \quad = \quad G(\mathbf{R}_1, \boldsymbol{\zeta_1}; s_a) G(\boldsymbol{\zeta_1}, \mathbf{R}_2; L - s_a) G(\mathbf{R_3}, \boldsymbol{\zeta_2}; \mathbf{s_b}) G(\boldsymbol{\zeta_2}, \mathbf{R}_4; L - s_b). \tag{3.28}$$

As it was done in the previous calculation, to obtain a partition function, the energy contribution of the tether between motor active heads and the work done by the active heads must be incorporated in (3.28) and an average has to performed over all possible spatial positions of the intermediate positions $\boldsymbol{\zeta}_1$ and $\boldsymbol{\zeta}_2$. Thus the partition function becomes

$$\begin{aligned}\mathcal{Z}(\{\mathbf{R}_i\}) &= \int_V d\boldsymbol{\zeta_1} \int_V d\boldsymbol{\zeta_2} G(\mathbf{0}, \boldsymbol{\zeta_1}; s_a) G(\boldsymbol{\zeta_1}, \mathbf{R}_0; L - s_a) G(\mathbf{R_1}, \boldsymbol{\zeta_2}; \mathbf{s_b}) G(\boldsymbol{\zeta_2}, \mathbf{R}_2; L - s_b) \\ &\times \exp\left(\frac{\beta k(\boldsymbol{\zeta_1} - \boldsymbol{\zeta_2})^2}{2} - \beta f L(s_a - s_a^0 + s_b - s_b^0)\right). \end{aligned} \tag{3.29}$$

The disorder averaged free energy is given by

$$\mathcal{F}(\Lambda) = \int P_c(\{\mathbf{R}_i\}) F_c(\{\mathbf{R}_i\}) \prod_{i=1} d\mathbf{R}_i = \int P_c(\{\mathbf{R}_i\}) \ln(\mathcal{Z}\{\mathbf{R}_i\}) \prod_{i=1} d\mathbf{R}_i. \tag{3.30}$$

The logarithm term in (3.30) can be expression as the coefficient of n, $A^n = 1 + n \ln A + O(n^2)$. As it was mentioned in the previous chapter, introducing this identity for the logarithm term in the free energy expression is equivalent to taking an annealed average of the replicated system. For the present network model, the network formation probability P_c can be written in terms of a formation hamiltonian similar in structure to the hamiltonian of the replicated systems. This shall conveniently be expressed as the zeroth replica coupled to the rest of replicas as it is commonly done in network theories [6].

3.3 Model Free Energy Calculation

For a system consisting of n_c networks in a medium, crosslinked as discussed, the total experimental free energy of the system can be expressed as:

$$\mathcal{F}(\Lambda) = \sum_{n_c} \int d\mathbf{R}_i e^{-\beta H^0(\{\mathbf{R}_i\})} \int \prod_{\alpha=1}^{n} d\mathbf{R}_i e^{-\beta \sum_\alpha^n H^\alpha(\{\mathbf{R}_i\})} \tag{3.31}$$

where H_0 is the hamiltonian for the zeroth replica and H^α is the hamiltonian of the replicated part of the system. As stated earlier, the partition function for the undeformed

copy of the system $\mathcal{Z}^0\left(\{\mathbf{R}_i\}_{i=1}^4\right)$, which is simply a sum over all available conformations, gives the probability P_c.

$$\begin{aligned}\mathcal{Z}^0\left(\{\mathbf{R}_i\}_{i=1}^4\right) &= \int_V d{\boldsymbol{\zeta_1}}^0 \int_V d{\boldsymbol{\zeta_2}}^0 \int_{\mathbf{r}_1^0=\mathbf{R}_1}^{\mathbf{r}_1^0(s_a)=\boldsymbol{\zeta_1^0}} \int_{\mathbf{r}_2^0(0)=\mathbf{R_2}}^{\mathbf{r}_2^0(L-s_a)=\boldsymbol{\zeta_1^0}} \int_{r_3^0=\mathbf{R}_3}^{\mathbf{r}_3^0(s_b)={\boldsymbol{\zeta_2}}^0} \\ &\times \int_{\mathbf{r}_4^0(0)=\mathbf{R}_4}^{\mathbf{r}_4(L-s_b)={\boldsymbol{\zeta_2}}^0} \prod_{\imath=1}^{4} \mathcal{D}\mathbf{r_i^0} \int ds_a \int ds_b e^{-\beta H(x^0,y^0,\{\mathbf{r}_i\}_{i=1}^4,s_a^0,s_b^0)} \\ &\times \delta(\mathbf{r}_1^0(s_a)-\mathbf{r}_2^0(L-s_a))\delta(\mathbf{r}_3^0(s_b)-\mathbf{r}_4^0(L-s_b)) \qquad (3.32)\end{aligned}$$

The delta functions impose the molecular motor crosslinking constraint as shown in FIG. 3.2. The fixed crosslinked topology of interest, is specified by demanding that the extreme end points of the chains are frozen at $\{\mathbf{R}_i\}_{i=1}^4$ with the active crosslink at some intermediate position $\{\boldsymbol{\zeta}_1,\boldsymbol{\zeta}_2\}$ along the respective chains. $H(s_a^0,s_b^0,{\boldsymbol{\zeta_1}}^0,{\boldsymbol{\zeta_2}}^0,\{\mathbf{r}_i^0\}_{i=1}^4)$ is the hamiltonian for the zeroth replica, a copy of the crosslinked system with inactive molecular motors, expressed as,

$$\begin{aligned}H(s_a^0,s_b^0,{\boldsymbol{\zeta_1}}^0,{\boldsymbol{\zeta_2}}^0,\{\mathbf{r}_i^0\}_{i=1}^4) &= -\frac{3}{2l}\sum_{i=1}^{2}\int_0^{L_i} ds_a^0\left(\frac{\partial\mathbf{r}_i^0}{\partial s_a^0}\right)^2 - \frac{3}{2l}\sum_{i=3}^{4}\int_0^{L_i} ds_b^0\left(\frac{\partial\mathbf{r}_i^0}{\partial s_b^0}\right)^2 \\ &- \frac{\beta k}{2}({\boldsymbol{\zeta_1}}^0-{\boldsymbol{\zeta_2}}^0)^2) \qquad (3.33)\end{aligned}$$

where the arc coordinate s_a^0 and $s_b^0 \in [0,L]$. $\beta = \frac{1}{k_BT}$, where k_B is Boltzmann constant and T is the temperature and ℓ is the kuhn length. The first two terms of the hamiltonian give the entropic contributions of each of the chains. The constituent chains segments are parameterised by a position vectors $\{\mathbf{r}_i(s_a^0)\}_{i=1}^2$ and $\{\mathbf{r}_i(s_b^0)\}_{i=3}^4$ respectively. This is because, for mathematical ease, each strand is assumed to be constituted by two substrands crosslinking at the position of the respective motor clustor heads such that $\mathbf{r}_1^0(L_1)=\mathbf{r}_2^0(0)$ and $\mathbf{r}_3^0(L_3)=\mathbf{r}_4^0(0)$ with $L=L_1+L_2=L_3+L_4$. The energetic contribution from the tether connecting the motor heads is added to the hamiltonian through the term $\frac{\beta k}{2}({\boldsymbol{\zeta_1}}^0-{\boldsymbol{\zeta_2}}^0)^2$.

When there is enough ATP in the system such that the molecular motors are active, in the presence of an external deformation, the partition function has a similar structure to the network formation probability but with contribution from activity. Thus the partition

function can be written as

$$\begin{aligned}\mathcal{Z}^{\alpha}(\{\Lambda\mathbf{R}_i\}_{i=1}^4) &= \int_V d{\boldsymbol{\zeta_1}}^{\alpha}\int_V d{\boldsymbol{\zeta_2}}^{\alpha}\int_{\mathbf{r}_1^{\alpha}(0)=\boldsymbol{\Lambda}R_0}^{\mathbf{r}_1^{\alpha}(s_a)={\boldsymbol{\zeta_1}}^{\alpha}}\int_{\mathbf{r}_2^{\alpha}(L)=\Lambda\mathbf{R}_2}^{\mathbf{r}_2^{\alpha}(L-s_a)=\boldsymbol{\zeta}_{\mathbf{1}}^{\alpha}}\int_{r_3^{\alpha}=\boldsymbol{\Lambda}\mathbf{R}_3}^{\mathbf{r}_2^{\alpha}(s_b)={\boldsymbol{\zeta_2}}^{\alpha}}\\ &\times \int_{\mathbf{r}_4^{\alpha}(0)=\boldsymbol{\Lambda}\mathbf{R}_4}^{\mathbf{r}_4(L-s_b^{\alpha})=\boldsymbol{\zeta}_{\mathbf{2}}^{\alpha}}\prod_{i=1}^{4}\mathcal{D}\mathbf{r}_i^{\alpha}\int_0^L s_a\int_0^L s_b\exp\left(-\beta H\left({\boldsymbol{\zeta_1}}^{\alpha},{\boldsymbol{\zeta_2}}^{\alpha},\{\mathbf{r}_i^{\alpha}\}_{i=1}^4,s_a^{\alpha},s_b^{\alpha},f\right)\right)\\ &\times \delta(\mathbf{r}^{\alpha}{}_1(s_a^{\alpha})-\mathbf{r}_2^{\alpha}(L-s_a^{\alpha}))\delta(\mathbf{r}_3(s_b^{\alpha})-\mathbf{r}_4^{\alpha}(L-s_b^{\alpha})),\end{aligned}\tag{3.34}$$

in this case $H(s_a^{\alpha},s_b^{\alpha},{\boldsymbol{\zeta_1}}^{\alpha},{\boldsymbol{\zeta_2}}^{\alpha},\{\mathbf{r}_i^{\alpha}\}_{i=1}^4,f)$ is the hamiltonian for a deformed copy of the system. It is similar to the hamiltonian for the zeroth replica but with the work done by the motor heads $\beta fL((s_a^{\alpha}-s_a^0)+(s_b^{\alpha}-s_b^0))$ incorporated. It is expressed as

$$\begin{aligned}H(s_a^{\alpha},s_b^{\alpha},{\boldsymbol{\zeta_1}}^{\alpha},{\boldsymbol{\zeta_2}}^{\alpha},\{\mathbf{r}_i^{\alpha}\}_{i=1}^4,f) &= -\frac{3}{2\ell}\sum_{i=1}^{2}\int_0^{L_i}ds_a^{\alpha}\left(\frac{\partial\mathbf{r}_i^{\alpha}}{\partial s_a^{\alpha}}\right)^2-\frac{3}{2l}\sum_{i=3}^{4}\int_0^{L_i}ds_b^{\alpha}\left(\frac{\partial\mathbf{r}_i^{\alpha}}{\partial s_b^{\alpha}}\right)^2\\ &- \frac{\beta k}{2}({\boldsymbol{\zeta_1}}^{\alpha}-{\boldsymbol{\zeta_2}}^{\alpha})^2+\beta fL((s_a^{\alpha}-s_a^0)+(s_b^{\alpha}-s_b^0)).\end{aligned}\tag{3.35}$$

As in the previous section, the subscript α is the replica index put in anticipation of the introducing of replicas. The disorder averaged free energy is thus given by:

$$\mathcal{F}=[F_c(\Lambda)]_d = -k_BT\frac{\int\prod_{i=1}^4 d\mathbf{R}_i\mathcal{Z}^0(\{\mathbf{R}_i\}_{i=1}^4)\ln(\mathcal{Z}^{\alpha}(\{\boldsymbol{\Lambda}\mathbf{R}_i\}_{i=1}^4))}{\int\prod_{i=1}^4 d\mathbf{R}_i\bar{\mathcal{Z}}^0(\{\mathbf{R}_i\}_{i=1}^4)}$$

where the waiting factor $\bar{\mathcal{Z}}^0$ is of similar structure to the zeroth replica partition function. The logarithm is generally not easy to integrate as indicated in section 3. The identity

$$[\ln(\mathcal{Z})]_d=\lim_{n\to 0}\frac{1}{n}([\mathcal{Z}^n]_d-1)\tag{3.36}$$

becomes extremely useful in disorder averaging the logarithm of the partition function. In above equation $[\cdots]_d$ denotes a disorder average over all copies of the system. The disorder

averaged partition function can be expressed as

$$
\begin{aligned}
[\mathcal{Z}^n(\Lambda)]_d \;=\; & \frac{1}{\mathcal{N}} \int \prod_{i=1}^{4} d\mathbf{R}_i \int_v d{\boldsymbol{\zeta_1}}^0 \int_v d{\boldsymbol{\zeta_2}}^0 \\
\times \; & \int_{\mathbf{r}_0^0(0)=\mathbf{R}_1}^{\mathbf{r}_1^0(s_a^0)={\boldsymbol{\zeta_1}}^0} \cdots \int_{\mathbf{r}_3^0(L)=\mathbf{R}_4}^{\mathbf{r}_3^0(L-s_b^0)={\boldsymbol{\zeta_2}}^0} \prod_{\imath=1}^{4} \mathcal{D}\mathbf{r}_i^0 \int_0^L ds_a^0 \int_0^L ds_b^0 e^{-\beta H({\boldsymbol{\zeta_1}}^0, {\boldsymbol{\zeta_2}}^0, \{\mathbf{r}_i^0\}, s_a^0, s_b^0)} \\
\times \; & \int \prod_{\alpha=1}^{n} d{\boldsymbol{\zeta_1}}^\alpha \int \prod_{\alpha=1}^{n} d{\boldsymbol{\zeta_2}}^\alpha \left[\int_{\mathbf{r}_0^\alpha(0)=\Lambda\mathbf{R}_1}^{\mathbf{r}_0^\alpha(s_a^\alpha)={\boldsymbol{\zeta_1}}^\alpha} \cdots \int_{\mathbf{r}_4^\alpha(L)=\boldsymbol{\Lambda}\mathbf{R}_4}^{\mathbf{r}_3^\alpha(L-s_b^\alpha)={\boldsymbol{\zeta_2}}^\alpha} \prod_{i=1}^{4} \prod_{\alpha=1}^{n} d\mathbf{r}_i^\alpha \int_0^L \prod_{\alpha=1}^{n} ds_a^\alpha \right. \\
\times \; & \left. \int_0^L \prod_{\alpha=1}^{n} ds_b^\alpha \; e^{-\beta \sum_\alpha^n H({\boldsymbol{\zeta_1}}^\alpha, {\boldsymbol{\zeta_2}}^\alpha, \{\mathbf{r}_i^\alpha\}, s_a^\alpha, s_b^\alpha, f)} \right] .
\end{aligned}
\tag{3.37}
$$

Upon evaluating the integrals over the position vectors $\mathbf{r}_i$ in (3.37), having conveniently expressed all the variables in non dimensional units, we obtain:

$$
\begin{aligned}
[\mathcal{Z}^n(\Lambda)]_d \;=\; & \frac{1}{\mathcal{N}} \int \prod_{i=1}^{4} d\mathbf{R}_i \\
\times \; & \left[\int_0^L \prod_{\alpha=0}^{n} ds_a^\alpha \int_0^L \prod_{\alpha=0}^{n} ds_b^\alpha \left(\frac{1}{3 + \beta k R_0^2 ((1-s_a^\alpha)s_a^\alpha + (1-s_b^\alpha)s_b^\alpha)} \right)^{\frac{3}{2}} \right. \\
\times \; & \left. \exp\left(-f_0(\{\mathbf{R}_i\}, s_a^0, s_b^0) - \sum_\alpha^n f_\alpha(\{\boldsymbol{\Lambda}\mathbf{R}_i\}, s_a^\alpha, s_b^\alpha, f) \right) \right]
\end{aligned}
\tag{3.38}
$$

See the appendix A.1 for an explicit expression for $f_0(\{\mathbf{R}_i\}_{i=1}^4, s_a^0, s_b^0)$ and $f_\alpha(\{\boldsymbol{\Lambda}\mathbf{R}_i\}_{i=1}^4, s_a^\alpha, s_b^\alpha, f)$. At this point we can implement a coordinate transformation in which the system is described in terms of the end-to-end distance of the connected strands $\mathbf{r}_1 = \mathbf{R}_2 - \mathbf{R}_1$, $\mathbf{r}_2 = \mathbf{R}_4 - \mathbf{R}_3$ and the difference and sum of the centers of mass of the connected strands: $\mathbf{r}_3 = c_1 - c_2$ and $\mathbf{r}_4 = c_1 + c_2$ respectively, where the centers of mass for the respective strands are denoted $c_1 = \frac{\mathbf{R}_1+\mathbf{R}_2}{2}$ and $c_2 = \frac{\mathbf{R}_3+\mathbf{R}_4}{2}$. Of course, the free energy does not depend on the sum of the centers of mass $\mathbf{r}_4$.

For more details about the resulting expressions after the transformation see the appendix A.1. The transformation allows us to express the equation (3.38) compactly in terms of a matrix of coefficients of the new coordinates

$$
\begin{aligned}
[\mathcal{Z}^n(\Lambda)]_d &= \frac{1}{\mathcal{N}} \int \prod_{\alpha=1} d\mathcal{R}_i \int_0^1 \prod_{\alpha=0}^{n} ds_a^\alpha \int_0^1 \prod_{\alpha=0}^{n} ds_b^\alpha \prod_{\alpha=0}^{n} \left(\frac{1}{W^\alpha}\right)^{\frac{3}{2}} \\
&\times \exp\left(-\frac{1}{2}\sum_{i=1}^{3} \mathcal{R}_i \left(\mathbf{M}^0 + \lambda_i^2 \sum_{\alpha=1}^{n} \mathbf{M}^\alpha\right) \mathcal{R}_i^\top\right) \\
&\times \exp\left(f\beta L n(s_a^0 + s_b^0) - \sum_{\alpha=1}^{n} f\beta L\,(s_a^\alpha + s_b^\alpha)\right). \qquad (3.39)
\end{aligned}
$$

In this equation $\mathcal{R}_i = (\mathbf{r}_{1,i}, \mathbf{r}_{3,i}, \mathbf{r}_{3,i})$ is a row vectors whose entries are the elements of the i'th cartesian coordinates of the new coordinates. The matrix $\mathbf{M}^0 + \lambda_i \sum_{\alpha=1}^{n} \mathbf{M}^\alpha$ is symmetric. $\mathbf{M}^0$ consists of coefficients originating from the zeroth replica while $\mathbf{M}^\alpha$ is a symmetric matrix consisting of coefficients originating from the replicated part of the system. $W^\alpha = 3 + \beta k R_0^2((1 - s_a^\alpha)s_a^\alpha) + (1 - s_b^\alpha)s_b^\alpha)$. At this stage the replica technique proves to be extremely handy as the integral over the disorder variables $\mathcal{R}_i$ can be dealt with first. Having performed the multidimensional Gaussian integral, we are left with an expression of the form

$$
\begin{aligned}
[\mathcal{Z}^n(\Lambda)]_d &= \frac{1}{\mathcal{N}} \int_0^1 \prod_{0}^{n} ds_a^\alpha \int_0^1 \prod_{0}^{n} ds_b^\alpha \left(\frac{1}{W_\alpha}\right)^{\frac{3}{2}} \frac{1}{\prod_{i=1}^{3} \sqrt{||\mathbf{M}^0 + \lambda_i^2 \sum_{\alpha=1}^{n} \mathbf{M}^\alpha||}} \\
&\times \exp\left\{-\sum_{\alpha=1}^{n} (\beta f L(s_a^\alpha + s_b^\alpha)) - (\beta f L n(s_a^0 + s_b^0))\right\} \\
&= \int_0^1 \prod_{0}^{n} ds_a^\alpha \int_0^1 \prod_{0}^{n} ds_b^\alpha \exp\left\{-\frac{1}{2}\sum_{i=1}^{3}\sum_{\alpha=0}^{n} (\ln(W_\alpha) + \operatorname{tr}\ln(\mathbf{M}^0 + \sum_{\alpha=0}^{n} \lambda_i^2 \mathbf{M}^\alpha)) \right. \\
&+ \left. (\beta f L n(s_a^0 + s_b^0) - \beta f L \sum_{\alpha=1}^{n} (s_a^\alpha + s_b^\alpha))\right\}. \qquad (3.40)
\end{aligned}
$$

3.3.1 Mean field Replica Saddle Point Approximation

Integrating over the trace of the logarithm in (3.40) is not practical as terms originating from the zeroth replica and higher replica couple in a non trivial way. This calls for introduction of a mean field saddle point approximation. Using saddle point approximation amounts to replacing the integral by its maximal contribution i.e replacing the integral by its stationary value with respect to the variation in (s_a, s_b). To simplify the notation, we

introduce a change of variables $s_a^\eta = t_\eta + \frac{1}{2}$ and $s_b^\eta = \tau_\eta + \frac{1}{2}$. In this case $\eta = 0$ for the zeroth replica and for higher replicas $\eta = \alpha$. To see how the rest of the terms are going to change refer to the appendix A.2. In terms of the transformed variables the exponential in equation (3.40)

$$\begin{aligned}\mathcal{G} &= \sum_{\alpha=0}^{n} \frac{3}{2} \ln(6 + \beta k R_0^2 (1 - 2t_\alpha^2 - 2\tau_\alpha^2)) + \frac{1}{2} \sum_{i=1}^{3} \mathrm{Tr} \ln((\mathbf{M}^0 + \sum_{\alpha=1}^{n} \lambda_i^2 \mathbf{M}^\alpha)) \\ &\quad + n\beta f L(t_0 + \tau_0) - \sum_{\alpha=1}^{n} \beta f L(t_\alpha + \tau_\alpha). \end{aligned} \tag{3.41}$$

For saddle-point

$$\left.\frac{\partial \mathcal{G}}{\partial t_\eta}\right|_{t_\eta^*, \tau_\eta^*} = 0 \quad \text{and} \quad \left.\frac{\partial \mathcal{G}}{\partial \tau_\eta}\right|_{t_\beta^*, \tau_\eta^*} = 0. \tag{3.42}$$

In general,

$$\begin{aligned}\left.\frac{\partial \mathcal{G}}{\partial t_\eta}\right|_{t_\eta^*, \tau_\eta^*} &= \frac{6\beta k R_0^2 t_\eta^*}{6 + km(1 - 2t_\eta^{*2} - 2\tau_\eta^{*2})} - \beta f L(n\delta_{\eta 0} + \sum_{\alpha}^{n} (1 - \delta_{\eta 0})) \\ &+ \frac{1}{2} \sum_{i=1}^{3} \mathrm{Tr} \left([\mathbf{M}_0^* + \lambda_i^2 \sum_{\alpha}^{n} \mathbf{M}_\alpha^*]^{-1} \frac{\partial \mathbf{M}}{\partial t_\eta} (\delta_{\eta 0} + \lambda_i^2 (1 - \delta_{\eta 0})) \right) \end{aligned} \tag{3.43}$$

and

$$\begin{aligned}\left.\frac{\partial \mathcal{G}}{\partial \tau_\eta}\right|_{t_\eta^*, \tau_\eta^*} &= \frac{6\beta k R_0^2 \tau_\eta^*}{6 + \beta k R_0^2 (1 - 2t_\eta^{*2} - 2\tau_\eta^{*2})} - \beta f L(n\delta_{\eta 0} + \sum_{\alpha=1}^{n} (1 - \delta_{\eta 0})) \\ &+ \frac{1}{2} \sum_{i=1}^{3} \mathrm{Tr} \left([\mathbf{M}_0^* + \lambda_i^2 \sum_{\alpha=1}^{n} \mathbf{M}_\alpha^*]^{-1} \frac{\partial \mathbf{M}}{\partial \tau_\eta} (\delta_{\eta 0} + \lambda_i^2 (1 - \delta_{\eta 0})) \right). \end{aligned} \tag{3.44}$$

3.3.2 Replica Symmetric Ansatz

Solving equation (3.43) and (3.44) for the zeros is still a challenge owing to the fact that we have a sum running over higher replica terms. One possible way of solving the equation is by introducing replica symmetric ansatz:

$$t_\eta = \begin{cases} t^* & ,\forall \eta > 0 \\ t_0^* & ,\eta = 0 \end{cases} \quad \text{and} \quad \tau_\eta = \begin{cases} \tau^* & ,\forall \eta > 0 \\ \tau_0^* & ,\eta = 0 \end{cases} .$$

Now for $\eta > 0$ the self consistency equation (3.43) becomes,

$$\begin{aligned} \left.\frac{\partial \mathcal{G}}{\partial t_\eta}\right|_{t^*,\tau^*} &= 0 = \frac{6\beta k R_0^2 t^*}{6 + \beta k R_0^2 (1 - 2t^{*2} - 2\tau^{*2})} - \beta f L n \\ &+ \frac{1}{2}\sum_{i=1}^{3} \mathrm{Tr}\left([\mathbf{M}_0^* + \lambda_i^2 n \mathbf{M}_\alpha^*]^{-1} \left.\frac{\partial \mathbf{M}}{\partial t_\eta}\right|_{t^*} \right). \end{aligned} \tag{3.45}$$

For $\eta = 0$ the self consistency equation (3.43) leads to,

$$\begin{aligned} \left.\frac{\partial \mathcal{G}}{\partial t_\eta}\right|_{t_{\eta^*},\tau_{\eta^*}} &= 0 = \frac{6\beta k R_0^2 t_0^*}{6 + \beta k R_0^2 (1 - 2t_0^{*2} - 2\tau_0^{*2})} + \beta f L n \\ &+ \frac{1}{2}\sum_{i=1}^{3} \mathrm{Tr}\left([\mathbf{M}_0^* + \lambda_i^2 n \mathbf{M}_\alpha^*]^{-1} \left.\frac{\partial \mathbf{M}}{\partial t_\eta}\right|_{t_0^*} \right). \end{aligned} \tag{3.46}$$

Similar equations in τ_η can be obtained under replica symmetric ansatz from the self consistency equation (3.43).

Reference system Equation

A sensible strategy is to switch off the motor force and external deformation by setting $f = 0$ and $\lambda_i = 1$ in the replica symmetric self consistency equation (3.45) and (3.46) obtaining what can be called the reference system equation. Demanding that the system is symmetric between the zeroth replica and higher replicas, in this case ($t_0^* = t^*, \tau_0^* = \tau^*$) in the reference system equation. We end up with a fully replica symmetric scenario for

the reference system:

$$\left.\frac{\partial \mathcal{G}}{\partial t}\right|_{t^*,\tau^*} = 0 = \frac{6\beta k R_0^2 t^*}{6+\beta k R_0^2(1-2t^{*2}-2\tau^{*2})} + \frac{3}{2}\mathrm{Tr}\left([(1+n)\widetilde{\mathbf{M}}]^{-1}\left.\frac{\partial \widetilde{\mathbf{M}}}{\partial t}\right|_{t^*}\right), \tag{3.47}$$

and

$$\left.\frac{\partial \mathcal{G}}{\partial \tau}\right|_{t^*,\tau^*} = 0 = \frac{6\beta k R_0^2 \tau^*}{6+\beta k R_0^2(1-2t^{*2}-2\tau^{*2})} + \frac{3}{2}\mathrm{Tr}\left([(1+n)\widetilde{\mathbf{M}}]^{-1}\left.\frac{\partial \widetilde{\mathbf{M}}}{\partial \tau}\right|_{\tau^*}\right), \tag{3.48}$$

where the matrix of coefficients for the most symmetric case $\widetilde{\mathbf{M}}$ becomes,

$$\widetilde{\mathbf{M}} = \begin{pmatrix} \frac{3}{2}\left(\frac{2\beta k t^2}{6+\beta k R_0^2(1-2t^2-2\tau^2)}+\frac{1}{R_0^2}\right) & \frac{6\beta k t\tau}{6+\beta k R_0^2(1-2t^2-2\tau^2)} & \frac{6\beta k t}{6+\beta k R_0^2(1-2t^2-2\tau^2)} \\ \frac{6\beta k t\tau}{6+\beta k R_0^2 R_0^2(1-2t^2-2\tau^2)} & \frac{3\left(\beta k R_0^2\left(2t^2-1\right)-6\right)}{2R_0^2\left(6+\beta k R_0^2(1-2t^2-2\tau^2)\right)} & -\frac{6\beta k\tau}{6+\beta k R_0^2(1-2t^2-2\tau^2)} \\ \frac{6\beta k t}{6+\beta k R_0^2(1-2t^2-2\tau^2)} & -\frac{6\beta k\tau}{6+\beta k R_0^2(1-2t^2-2\tau^2)} & \frac{3\beta k}{6+\beta k R_0^2(1-2t^2-2\tau^2)} \end{pmatrix}. \tag{3.49}$$

The exact values for the t^* and τ^* at the minima or at the maximal contributions are obtained by solving the fully symmetric case self consistency equation (3.47) and (3.48) for the reference system obtaining the following extrema coordinates for the system:

$$\{t^*=0,\tau^*=0\} \quad \text{and}$$
$$\left\{ t^* = -\pm\frac{1}{2}\sqrt{-\frac{(6+\beta k R_0^2)\left(11-31n\pm\sqrt{121-178n+121n^2}\right)}{42\beta k R_0^2 n}}\,, \right.$$
$$\left. \tau^* = -\pm\frac{1}{2}\sqrt{-\frac{(6+\beta k R_0^2)\left(11-31n\pm\sqrt{121-178n+121n^2}\right)}{42\beta k R_0^2 n}} \right\}.$$

For expressions leading to above extrema points see appendix A.3. It turns out that the origin (0,0) is a global minimum for the system since for all $(t,\tau)\in[-\frac{1}{2},\frac{1}{2}]$, $\mathcal{G}((t^*,\tau^*)=(0,0))\leq\mathcal{G}(t,\tau)$.

Perturbative Approach

We are interested in an expression for the free energy of the system when the molecular motor force is switched on in the presence of external deformation. To achieve this we employ a perturbative approach for small motor force. We assume that the respective minima coordinates, associated with the deformed system, will shift by small factor ϵ_1 and ϵ_2 depending on the motor force and the external deformation, i.e $\widetilde{t}^* = t^* + \epsilon_1$ and $\widetilde{\tau}^* = \tau^* + \epsilon_2$. There is no shift in the minima associated with the undeformed systems, t_0^* and τ_0^*, solving equation (3.45) and (3.46) simultaneously for ϵ_1 and ϵ_2 we obtain,

$$\epsilon_1 = \epsilon_2 = \frac{f(6+\beta k R_0^2)\beta\left(1+2\sum_{i=1}^{3}\lambda_i^2\right)}{6\beta k R_0^2}. \tag{3.50}$$

At the shifted global minimum the disorder averaged partition function without fluctuations can be expressed as $[\mathcal{Z}^n]_d = \frac{1}{\mathcal{N}}\exp\left(-\mathcal{G}(\widetilde{t}_\alpha^*, \widetilde{\tau}_\alpha^*, t_0^*, \tau_0^*)\right)$

Up to first order in the replica index n, the disorder averaged partition function becomes

$$\begin{aligned}[\mathcal{Z}^n]_d &= \frac{1}{\mathcal{N}}\exp\left(-\frac{3}{2}\left(\ln\left[\frac{54k\beta}{R_0^4}\right] + n\left(3\sum_{i=1}^{3}\lambda_i^2 + \ln\left[6+k\beta R_0^2\right]\right)\right)\right. \\ &- \left.\frac{f^2L^2n\beta\left(1+2\sum_{i=1}^{3}\lambda_i^2\right)(6+k\beta R_0^2)}{3kR_0^2}\right),\end{aligned} \tag{3.51}$$

where the nomalization factor $\mathcal{N}$ is given by

$$\mathcal{N} = \exp\left(-\frac{3}{2}\ln\left[\frac{54k\beta}{R_0^4}\right]\right). \tag{3.52}$$

Then

$$[\mathcal{Z}^n]_d - 1 = -\left(\frac{3n}{2}\left(3\sum_{i=1}^{3}\lambda_i^2 + \ln\left[6+k\beta R_0^2\right]\right) + \frac{f^2L^2n\beta\left(1+2\sum_{i=1}^{3}\lambda_i^2\right)(6+k\beta R_0^2)}{3kR_0^2}\right).$$

Upon taking the replica limit in the above expression and multiplying the resulting expression by the global temperature for the system, the free energy is found to be

$$\mathcal{F} = k_B T \left(\frac{3}{2} \left(3 \sum_{i=1}^{3} \lambda_i^2 + \ln \left[6 + k\beta R_0^2 \right] \right) + \frac{f^2 L^2 \beta \left(1 + 2\lambda_i^2 \right) \left(6 + k\beta R_0^2 \right)}{3kR_0^2} \right).$$

If the system is subjected to an isovolumetric deformation along the x-axis, tension on the network strands is given by

$$T_x / k_B T = 9 \left(\lambda_1 - \frac{1}{\lambda_1^2} \right) + \frac{f^2 L^2 \beta \left(\lambda_1 - \frac{1}{\lambda_1^2} \right) \left(6 + k\beta R_0^2 \right)}{3kR_0^2}. \tag{3.53}$$

and the hydrostatic pressure balancing the force becomes

$$\mathcal{P} / k_B T = 9 \left(\frac{1}{\lambda_1^3} - \frac{1}{\lambda_1^6} \right) + \frac{f^2 L^2 \beta \left(2 \left(\frac{1}{\lambda_1^3} - \frac{1}{\lambda_1^6} \right) \left(6 + k\beta \ R_0^2 \right) \right)}{3kR_0^2}. \tag{3.54}$$

We conclude that there is a positive $(fL\beta)^2$ contribution to the network tension T_x and pressure P as seen in equation (3.26). Just like in the single strand model with disorder, we realise that the tension (3.53) and the pressure balancing the tension equation (3.54) depend on the molecular motor force. This dependence is a modification to the normal tension and pressure that could be obtained in the absence of the motor force. From this we learn that force generated by the molecular motor enhance the internal contraction of the network subject to a uniaxial isovolumentic deformation. An outline of the replica calculation with fluctuations is presented in the appendix (A.4).

Chapter 4

Conclusion and Outlook

We developed a model for a network of actin filaments crosslinked by active crosslinkers (molecular motor clusters) based on the slipping link model analogy. The central aim of this work was to construct a theory that explains the role active crosslinking molecular motor proteins play in the mechanical properties of cells in living systems. The model calculations were performed based on the following assumptions:

- The network was assumed to be consisting of strands of length L and molecular motor mobile crosslinkers of the same size and strength.
- The network chains were assumed to be long enough as compared to the chain persistence length, $L \gg \ell_p$, such that it was sensible to model the network chains as Gaussian.
- The network was considered to be well into galation phase and the network chains were assumed to be phantom in nature. As a result chains could intersect each other and the possibility of excluded volume and entanglements were ignored.

The network elastic response calculations in chapter 2 are studied using a single chain picture typical of classical rubber elasticity [33]. The chapter introduced the concept of mobile active crosslinks and set the scene, in terms of path integral approach [34] and saddle point approximation, for a model of high complexity as presented in the subsequent chapters. We learned that the elastic response for the network can be classified according to

regimes characterised by extension between fixed crosslinkers. These are a high extension regime, moderate extension and low extension regime, in which the active crosslink reaches the network end points. For the high extension regimes, there is a good agreement between the analytical and the numerical results for the network elastic response obtained. For the moderate stretching regime and the regime when the motor is aligned towards the end points, the network elastic response is over estimated by analytical results as compared to the numerical results. However, the trends typical of each regime were found to be comparable. The internal tension on the network strand for the high stretching regime and for the regime when the mobile crosslink is aligned towards the end points obey Hooke's law for a simple spring. In general the elastic response of a single stranded network suggested a possibility of hysteresis with increasing network end points extension.

The first part of chapter 3 captured the concept of disorder using a single strand model idea similar to the one in chapter 2 but in a three dimensional setting. The quenched disorder originates from the random permanent anchoring of the network strand to the affine background. In this calculation, we demonstrated that disorder can be dealt with mathematically by utilizing the replica technique. A mean field approximation was used to make the free energy calculation tractable.

In the last part of chapter 3, an extension of the normal slip link model [4,12] to incorporate mobile active crosslinks, is presented. The disorder in this model, is dealt with by invoking the replica trick as done in the preceding calculation. The replica symmetry breaking is assumed between the zeroth and higher replica sector. For the high replica sector, $\alpha > 0$, the replicas are assumed to be symmetric. Saddle point approximation in a mean field theory context is utilised in order to get an approximation of the partition function for the system. From the first model calculations in chapter 3, we found that the elastic response of the network subjected to a uniaxial isovolumetric deformation is given by the expression,

$$T_x = k_B T \left(\lambda_1 - \frac{1}{\lambda_1^2}\right)\left(\frac{1}{18}\left(18 + \beta k R_0^2\right) + \frac{1}{432}\left(72 + 5k\beta R_0^2\right)(\beta f L)^2\right). \tag{4.1}$$

and for the two stranded model

$$T_x = k_B T \left(\lambda_1 - \frac{1}{\lambda_1^2}\right)\left(9 + \frac{2f^2L^2\beta\left(6 + k\beta R_0^2\right)}{3kR_0^2}\right). \tag{4.2}$$

In both model calculations, in addition to the normal network elasticity, we obtain an extra term in which the deformation is modified by a factor depending on the ratio of the spring constant of the chain to the spring constant of the molecular motor tether. This factor is coupled to the molecular motor force f^2 . From equations (4.1) and (4.2) we see that the molecular motor force bring a positive contribution to the network internal contraction force T_x. A similar contribution is obtained for the hydrostatic pressure $\mathcal{P}$, balancing the network tension. Hence we conclude that the force generated by molecular motors leads to more internal network contraction.

We learned that modelling the network components as Gaussian chains provide a huge mathematical simplification and some important insights into the physical properties of active networks. For future work the three dimensional models presented here shall be extended to include the treatment of actin networks as semiflexible chains. We employ a replica symmetric ansatz. However, given the nature of the zeroth replica, there must be a difference in the saddle-point for the zeroth and higher replicas - but this does not correspond to replica symmetry breaking in the usual terminology, since all replicas with force are still treated symmetrically. A more accurate development of the theory should consider full replica symmetry breaking for all replicas. The theory presented here is valid only for small molecular motor force, further improvement could be made by considering an arbitrary molecular motor force. Left to separate research are the predictions of the analytical results which could be tested against experiments and simulation work.

Appendix A

A.1 System Coordinate Transformation

$$\begin{aligned} f_0(\{\mathbf{R}_j\}, s_a^0, s_b^0, \phi) &= 3\left(s_b^0\left(\beta k R_0^2\left(s_a^0\left(-\mathbf{R}_4 s_a^0 - \mathbf{R}_2 s_b^0 + \mathbf{R}_2 + \mathbf{R}_4\right) + \mathbf{R}_1\left(1-s_a^0\right)\left(1-s_b^0\right)\right) + 3\mathbf{R}_4\right)\right. \\ &+ \left.\mathbf{R}_3\left(1-s_b^0\right)\left(3+\beta k R_0^2 s_a^0\left(1-s_a^0\right)\right)\right)^2 / \blacksquare_0 \\ &+ \frac{9\left(2\mathbf{R}_1\left(\mathbf{R}_1+\mathbf{R}_2\right)s_a^0 + \left(\mathbf{R}_1-\mathbf{R}_2\right)^2 s_a^{o2} + \mathbf{R}_1^2\right)}{2R_0^2\left(1-s_a^0\right)s_a^0\left(3+\beta k R_0^2 s_a^0\left(1-s_a^0\right)\right)} \\ &+ \frac{3\mathbf{R}_1^2}{2R_0^2 s_a^0} + \frac{3\mathbf{R}_2^2}{2R_0^2\left(1-s_a^0\right)} + \frac{3\mathbf{R}_3^2}{2R_0^2 s_b^0} + \frac{3\mathbf{R}_4^2}{2R_0^2\left(1-s_b^0\right)} \end{aligned} \tag{A.1}$$

where the deviding

$$\blacksquare_0 = 2R_0^2\left(1-s_b^0\right)s_b^0\left(\beta k R_0^2 s_a^0\left(1-s_a^0\right)\right)\left(3+\beta k R_0^2\left(\left(1-s_a^0\right)s_a^0 + \left(1-s_b^0\right)s_b^0\right)\right) \tag{A.2}$$

and

$$\begin{aligned} & f_\alpha(\{\mathbf{\Lambda R}_j\}, s_a^\alpha, s_b^\alpha, \phi) \\ = \;& 3\left(s_b^\alpha\left(\beta k R_0^2\left(s_a^\alpha\left(-\mathbf{\Lambda R}_4 s_a^\alpha - \mathbf{\Lambda R}_2 s_b^\alpha + \mathbf{\Lambda R}_2 + \mathbf{\Lambda R}_4\right) + \mathbf{\Lambda R}_1\left(s_a^\alpha - 1\right)\left(s_b^\alpha - 1\right)\right) + 3\mathbf{\Lambda R}_4\right)\right. \\ + \;& \left.\mathbf{\Lambda R}_3\left(1-s_b^\alpha\right)\left(3+\beta k R_0^2 s_a^\alpha\left(s_a^\alpha - 1\right)\right)\right)^2 / \blacksquare_\alpha \\ + \;& \frac{9\left(2\mathbf{\Lambda R}_1\left(\mathbf{\Lambda R}_1 + \mathbf{\Lambda R}_2\right)s_a^\alpha + \left(\mathbf{\Lambda R}_1 - \mathbf{\Lambda R}_2\right)^2 s_a^{\alpha 2} + \mathbf{\Lambda^2 R}_1^2\right)}{2R_0^2\left(1-s_a^\alpha\right)s_a^\alpha\left(3+\beta k R_0^2 s_a^\alpha\left(1-s_a^\alpha\right)\right)} \\ + \;& \frac{3\mathbf{\Lambda^2 R}_1^2}{2R_0^2 s_a^\alpha} + \frac{3\mathbf{\Lambda^2 R}_2^2}{2R_0^2\left(1-s_a^\alpha\right)} + \frac{3\mathbf{\Lambda^2 R}_3^2}{2R_0^2 s_b^\alpha} + \frac{3\mathbf{\Lambda^2 R}_4^2}{2R_0^2\left(1-s_b^\alpha\right)} \end{aligned} \tag{A.3}$$

where we denote

$$\blacksquare_\alpha = 2R_0^2\left(1-s_b^\alpha\right)s_b^\alpha\left(3+\beta k R_0^2 s_a^\alpha\left(1-s_a^\alpha\right)\right)\left(3+\beta k R_0^2\left(\left(1-s_a^\alpha\right)s_a^\alpha + \left(1-s_b^\alpha\right)s_b^\alpha\right)\right). \tag{A.4}$$

Once the system is represented in terms of the end-to-end distance and the difference of centers of mass variables the exponential terms involving the high replica sector becomes

$$\begin{aligned}\widetilde{f}_{\alpha} &= \frac{3}{8}\mathbf{r}_1^2 k\left(\frac{(\mathbf{\Lambda}-2\mathbf{\Lambda}s_a^{\alpha})^{\,2}}{3+\beta k R_0^2\left((1-s_a^{\alpha})\,s_a^{\alpha}+\left(1-s_b^{\alpha}\right)s_b^{\alpha}\right)}+\frac{4\mathbf{\Lambda}^2}{R^2}\right)+\frac{3}{2}k\mathbf{r}_2\mathbf{r}_1\left(\frac{\mathbf{\Lambda}^2\left(1-2s_a^{\alpha}\right)\left(1-2\,s_b^{\alpha}\right)}{3+\beta k R_0^2\left((1-s_a^{\alpha})\,s_a^{\alpha}+\left(1-s_b^{\alpha}\right)s_b^{\alpha}\right)}\right)\\ &+\frac{3k}{8R^2}\mathbf{r}_2^2\mathbf{\Lambda}^2\left(\frac{4R^2\left(1-s_a^0\right)s_a^0+\beta k R_0^2+12}{3+\beta k R_0^2\left((1-s_a^0)\,s_a^0+\left(1-s_b^0\right)s_b^0\right)}\right)+\frac{3}{2}k\mathbf{r}_3^2\left(\frac{\mathbf{\Lambda}^2}{3+\beta k R_0^2\left((1-s_a^{\alpha})\,s_a^{\alpha}+\left(1-s_b^{\alpha}\right)s_b^{\alpha}\right)}\right)\\ &3k\mathbf{r}_1\mathbf{r}_3\left(\frac{\mathbf{\Lambda}^2\left(1-2s_a^{\alpha}\right)}{3+\beta k R_0^2\left((1-s_a^{\alpha})\,s_a^{\alpha}+\left(1-s_b^{\alpha}\right)s_b^{\alpha}\right)}\right)-3k\mathbf{r}_2\mathbf{r}_3\left(\frac{\mathbf{\Lambda}^2\left(1-2s_b^{\alpha}\right)}{3+\beta k R_0^2\left((1-s_a^{\alpha})\,s_a^{\alpha}+\left(1-s_b^{\alpha}\right)s_b^{\alpha}\right)}\right),\end{aligned}\tag{A.5}$$

while for the zeroth replica the exponential terms becomes

$$\begin{aligned}\widetilde{f}_{0} &= \frac{3}{8}\mathbf{r}_1^2\left(\frac{k\left(1-2s_a^0\right)^{\,2}}{3+\beta k R_0^2\left((1-s_a^0)\,s_a^0+\left(1-s_b^0\right)s_b^0\right)}-\frac{4}{R^2}\right)+\frac{3}{2}k\mathbf{r}_2\mathbf{r}_1\left(\frac{\left(1-2s_a^0\right)\left(1-2s_b^0\right)}{3+\beta k R_0^2\left((1-s_a^0)\,s_a^0+\left(1-s_b^0\right)s_b^0\right)}\right)\\ &+\frac{3}{8R^2}\mathbf{r}_2^2\left(\frac{4\beta k R_0^2\left(1-s_a^0\right)s_a^0+\beta k R_0^2+12}{3+\beta k R_0^2\left((1-s_a^0)\,s_a^0+\left(1-s_b^0\right)s_b^0\right)}\right)+\frac{3}{2}k\mathbf{r}_3^2\left(\frac{1}{3+\beta k R_0^2\left((1-s_a^0)\,s_a^0+\left(1-s_b^0\right)s_b^0\right)}\right)\\ &3k\mathbf{r}_1\mathbf{r}_3\left(\frac{1-2s_a^0}{\left(3+\beta k R_0^2\left((1-s_a^0)\,s_a^0+\left(1-s_b^0\right)s_b^0\right)\right)}\right)-3\mathbf{r}_2\mathbf{r}_3\left(\frac{k\left(1-2s_b^0\right)}{3+\beta k R_0^2\left((1-s_a^0)\,s_a^0+\left(1-s_b^0\right)s_b^0\right)}\right).\end{aligned}\tag{A.6}$$

As we can see from the above expressions, the system does not depend on the sum of the centers of mass of the connected strands rather it depends on their differences. The above equations can be expressed as a product of a row vector $\mathbf{R}_i = (\mathbf{r}_{1,i}, \mathbf{r}_{2,i}, \mathbf{r}_{3,i})$ and a column a vector $\mathcal{R}_i^{\top}$. Where $\mathbf{R}_i$ is the i-th component of $\mathbf{R} = (\mathbf{r}_1, \mathbf{r}_2, \mathbf{r}_3)$. The coefficients $\mathbf{M} = \mathbf{M}^0 + \lambda_i^2 \sum_1^n \mathbf{M}^{\alpha}$, where

$$\mathbf{M}^0 = \begin{pmatrix} \frac{3k\left(1-2\,s_a^0\right)^2}{3+\beta k R_0^2\left((1-s_a^o)s_a^0+\left(1-s_b^0\right)s_b^0\right)}+\frac{3}{R_0^2} & \frac{-3k\left(1-2s_a^0\right)\left(1-2s_b^0\right)}{2\left(3+\beta k R_0^2\left((1-s_a^0)s_a^0+\left(1-s_b^0\right)s_b^0\right)\right)} & \frac{3k\left(1-2s_a^0\right)}{\left(3+\beta k R_0^2\left((1-s_a^0)s_a^0+\left(1-s_b^0\right)s_b^0\right)\right)} \\ \frac{-3k\left(1-2s_a^0\right)\left(1-2s_b^0\right)}{2\left(3+\beta k R_0^2\left((1-s_a^0)s_a^0+\left(1-s_b^0\right)s_b^0\right)\right)} & \frac{3\left(4\beta k R_0^2\left(1-s_a^0\right)s_a^0+\beta k R_0^2+12\right)}{4R^2\left(3+\beta k R_0^2\left((1-s_a^0)s_a^0+\left(1-s_b^0\right)s_b^0\right)\right)} & \frac{-3k\left(1-2s_b^0\right)}{\left(3+\beta k R_0^2\left((1-s_a^0)s_a^0+s_b^0\left(1-s_b^0\right)\right)\right)} \\ \frac{3k\left(1-2s_a^0\right)}{3+\beta k R_0^2\left((1-s_a^0)s_a^0+\left(1-s_b^0\right)s_b^0\right)} & \frac{-3k\left(1-2s_b^0\right)}{3+\beta k R_0^2\left((1-s_a^0)s_a^0+\left(1-s_b^0\right)s_b^0\right)} & \frac{3k}{3+\beta k R_0^2\left((1-s_a^0)s_a^0+\left(1-s_b^0\right)s_b^0\right)} \end{pmatrix}\tag{A.7}$$

and

$$\mathbf{M}^{\alpha} = \begin{pmatrix} \frac{3k(1-2s_a^{\alpha})^2}{3+\beta k R_0^2\left((1-s_a^{\alpha})s_a^{\alpha}+\left(1-s_b^{\alpha}\right)s_b^{\alpha}\right)}+\frac{3}{R_0^2} & \frac{-3k\,\left(1-2s_a^{\alpha}\right)\left(1-2s_b^{\alpha}\right)}{2\left(3+\beta k R_0^2\left((1-s_a^{\alpha})s_a^{\alpha}+\left(1-s_b^{\alpha}\right)s_b^{\alpha}\right)\right)} & \frac{3k\,\left(1-2s_a^{\alpha}\right)}{3+\beta k R_0^2\left((1-s_a^{\alpha})s_a^{\alpha}+\left(1-s_b^{\alpha}\right)s_b^{\alpha}\right)} \\ \frac{-3\,k(1-2s_a^{\alpha})\left(1-2s_b^{\alpha}\right)}{2\left(3+\beta k R_0^2\left((1-s_a^{\alpha})s_a^{\alpha}+\left(1-s_b^{\alpha}\right)s_b^{\alpha}\right)\right)} & \frac{3\left(4\beta k R_0^2(1-s_a^{\alpha})s_a^{\alpha}+\beta k R_0^2+12\right)}{4R^2\left(3+\beta k R_0^2\left((1-s_a^{\alpha})s_a^{\alpha}+\left(1-s_b^{\alpha}\right)s_b^{\alpha}\right)\right)} & \frac{-3k\,\left(1-2s_b^{\alpha}\right)}{3+\beta k R_0^2\left((1-s_a^{\alpha})s_a^{\alpha}+s_b^{\alpha}\left(1-s_b^{\alpha}\right)\right)} \\ \frac{3k\,\left(1-2s_a^{\alpha}\right)}{3+\beta k R_0^2\left((1-s_a^{\alpha})s_a^{\alpha}+\left(1-s_b^{\alpha}\right)s_b^{\alpha}\right)} & \frac{-3k\,\left(1-2s_b^{\alpha}\right)}{2\left(3+\beta k R_0^2\left((1-s_a^{\alpha})s_a^{\alpha}+\left(1-s_b^{\alpha}\right)s_b^{\alpha}\right)\right)} & \frac{3k}{3+\beta k R_0^2\left((1-s_a^{\alpha})s_a^{\alpha}+\left(1-s_b^{\alpha}\right)s_b^{\alpha}\right)} \end{pmatrix}.\tag{A.8}$$

A.2 Change of Variables

After the change of variables, $s_\alpha \to \tau_\alpha$ $\mathbf{M}^0$ and $\mathbf{M}^\alpha$ becomes $\mathcal{M}^0$ and $\mathcal{M}^\alpha$ respectively where

$$\mathcal{M}_0 = \begin{pmatrix} \frac{6kt_0^2}{6+\beta kR_0^2\left(1-\left(2t_0^2+2\tau_0^2\right)\right)} + \frac{3}{2R_0^2} & -\frac{12kt_0\tau_0}{6+\beta kR_0^2\left(1-\left(2t_0^2+2\tau_0^2\right)\right)} & -\frac{12kt_0}{6+\beta kR_0^2\left(1-\left(2t_0^2+2\tau_0^2\right)\right)} \\ -\frac{12kt_0\tau_0}{6+\beta kR_0^2\left(1-\left(2t_0^2+2\tau_0^2\right)\right)} & \frac{\beta kR_0^2\left(3-6t_0^2\right)+18}{R^2\left(6+\beta kR_0^2\left(1-\left(2t_0^2+2\tau_0^2\right)\right)\right)} & \frac{12k\tau_0}{6+\beta kR_0^2\left(1-\left(2t_0^2+2\tau_0^2\right)\right)} \\ -\frac{12kt_0}{6+\beta kR_0^2\left(1-\left(2t_0^2+2\tau_0^2\right)\right)} & \frac{12k\tau_0}{6+\beta kR_0^2\left(1-\left(2t_0^2+2\tau_0^2\right)\right)} & \frac{6k}{6+\beta kR_0^2\left(1-\left(2t_0^2+2\tau_0^2\right)\right)} \end{pmatrix} \tag{A.9}$$

and

$$\mathcal{M}_\alpha = \begin{pmatrix} \frac{3}{R^2} + \frac{6kt_\alpha^2}{6+\beta kR_0^2(1-(2t_\alpha^2+2\tau_\alpha^2))} & -\frac{12kt_\alpha\tau_\alpha}{6+\beta kR_0^2(1-(2t_\alpha^2+2\tau_\alpha^2))} & -\frac{12kt_\alpha}{6+\beta kR_0^2(1-(2t_\alpha^2+2\tau_\alpha^2))} \\ -\frac{12kt_\alpha\tau_\alpha}{6+\beta kR_0^2(1-(2t_\alpha^2+2\tau_\alpha^2))} & \frac{\beta kR_0^2\left(3-6t_\alpha^2\right)+18}{R_0^2\left(6+\beta kR_0^2(1-(2t_\alpha^2+2\tau_\alpha^2))\right)} & \frac{12k\tau_\alpha}{6+\beta kR_0^2(1-(2t_\alpha^2+2\tau_\alpha^2))} \\ -\frac{12kt_\alpha}{6+\beta kR_0^2(1-(2t_\alpha^2+2\tau_\alpha^2))} & \frac{12k\tau_\alpha}{6+\beta kR_0^2(1-(2t_\alpha^2+2\tau_\alpha^2))} & \frac{6k}{6+\beta kR_0^2(1-(2t_\alpha^2+2\tau_\alpha^2))} \end{pmatrix}. \tag{A.10}$$

The transformed W_0 and W_α becomes $3+\frac{1}{2}\beta kR_0^2\left(1-(2t_0^2+2\tau_0^2)\right)$ and $3+\frac{1}{2}\beta kR_0^2\left(1-(2t_\alpha^2+2\tau_\alpha^2)\right)$ respectively.

A.3 Solving for the extrema

For the fully replica symmetric case $\mathcal{G}$ becomes

$$\mathcal{G} = \frac{3}{2}\left(\ln\left(6+\beta kR_0^2\left(1-2t^2-2\tau^2\right)\right)\right) - \frac{9}{2}\left(\ln(\left(6+\beta kR_0^2\left(1-2t^2-2\tau^2\right)\right)\right) + \frac{3}{2}\mathrm{Tr}[\ln(\mathbf{M})]. \tag{A.11}$$

and the matrix of coefficients $\mathbf{M}$ simplifies to

$$\mathbf{M} = \frac{(n+1)}{6+\beta kR_0^2\left(1-2t^2-2\tau^2\right)} \begin{pmatrix} \frac{3\left(\beta kR_0^2\left(2\tau^2-1\right)-6\right)}{2R_0^2} & 6kt\tau & 6kt \\ 6kt\tau & \frac{3\left(\beta kR_0^2\left(2t^2-1\right)-6\right)}{2R_0^2} & -6k\tau \\ 6kt & -6k\ \tau & -3k \end{pmatrix}. \tag{A.12}$$

This allows us to write the reference system minimization equations as

$$\begin{aligned}\frac{\partial \mathcal{G}}{\partial t} &= -3\frac{\partial}{\partial t}\left(\ln\left(6+\beta k R_0^2\left(1-2t^2-2\tau^2\right)\right)\right)+\frac{3}{2(n+1)}\mathrm{Tr}\left[\widetilde{\mathbf{M}}^{-1}.\frac{\partial}{\partial t}\left(\widetilde{\mathbf{M}}\right)\right]\\ &= \frac{6\beta k R_0^2 t\left(\beta k R_0^2\left(16t^2+26\tau^2-5\right)-30\right)}{(n+1)\left(\beta^2k^2R_0^4\left(16t^4+2t^2\left(26\tau^2-5\right)+16\tau^4-10\tau^2+1\right)-12\beta k R_0^2\left(5t^2+5\tau^2-1\right)+36\right)}\\ &\quad+\frac{12\beta k R_0^2 t}{\beta k R_0^2\left(-2t^2-2\tau^2+1\right)+6}=0 \end{aligned} \tag{A.13}$$

and

$$\begin{aligned}\frac{\partial \mathcal{G}}{\partial \tau} &= -3\frac{\partial}{\partial \tau}\left(\ln\left(6+\beta k R_0^2\left(1-2t^2-2\tau^2\right)\right)\right)+\frac{3}{2(n+1)}\mathrm{Tr}\left[\widetilde{\mathbf{M}}^{-1}.\frac{\partial}{\partial \tau}\left(\widetilde{\mathbf{M}}\right)\right]\\ &= \frac{6\beta k R_0^2 \tau\left(\beta k R_0^2\left(16t^2+26\tau^2-5\right)-30\right)}{(n+1)\left(\beta^2k^2R_0^4\left(16t^4+2t^2\left(26\tau^2-5\right)+16\tau^4-10\tau^2+1\right)-12\beta k R_0^2\left(5t^2+5\tau^2-1\right)+36\right)}\\ &\quad+\frac{12\beta k R_0^2 \tau}{\beta k R_0^2\left(-2t^2-2\tau^2+1\right)+6}=0. \end{aligned} \tag{A.14}$$

In this case $\widetilde{\mathbf{M}}$ is the matrix that remain when common terms are factored out. As it can be seen in equation (A.12), solving the equation (A.13) and (A.14) simultaneously, we obtain the minima points

$$\begin{aligned}&\{t^*=0,\tau^*=0\} \quad \text{and}\\ &\left\{\begin{aligned} t^* &= -\pm\frac{1}{2}\sqrt{-\frac{\left(6+\beta k R_0^2\right)\left(11-31n\pm\sqrt{121-178n+121n^2}\right)}{42\beta k R_0^2 n}}\,,\\ \tau^* &= -\pm\frac{1}{2}\sqrt{-\frac{\left(6+\beta k R_0^2\right)\left(11-31n\pm\sqrt{121-178n+121n^2}\right)}{42\beta k R_0^2 n}}\end{aligned}\right\}\end{aligned} \tag{A.15}$$

and the maxima the maxima points

$$\left\{t=\pm\frac{\sqrt{(6+\beta kR_0^2)(-3+5n)}}{4\sqrt{\beta kR_0^2 n}},\tau=0\right\},\left\{\tau\pm\frac{\sqrt{(6+\beta kR_0^2)(-3+5n)}}{4\sqrt{\beta kR_0^2 n}},t=0\right\},$$
$$\left\{t=\pm\frac{1}{2\sqrt{\frac{42\beta kR_0^2 n}{(6+\beta kR_0^2)\left(-11+31n+\sqrt{121-178n+121n^2}\right)}}},\tau=\pm\frac{1}{2\sqrt{\frac{42\beta kR_0^2 n}{(6+\beta kR_0^2)\left(-11+31n+\sqrt{121-178n+121n^2}\right)}}}\right\}. \tag{A.16}$$

A.4 Outline of the replica calculation with fluctuations included

Upon considering fluctuations about the minimum solution

$$\mathcal{G}\approx\mathcal{G}(\widetilde{t}^*_\alpha,\widetilde{\tau}^*_\alpha,t_0^*,\tau_0^*)+\left(\begin{array}{cccc}t_\alpha-\widetilde{t}^*_\alpha, & \tau_\alpha-\widetilde{\tau}^*_\alpha, & t_0-t_0^*, & \tau_0-\tau_0^*\end{array}\right)F_1\left(\begin{array}{c}t_\alpha-\widetilde{t}^*_\alpha\\ \tau_\alpha-\widetilde{\tau}^*_\alpha\\ t_0-t_0^*\\ \tau_0-\tau_0^*\end{array}\right)+O(3) \tag{A.17}$$

where F_1 is a matrix of the form

$$F_1=\left(\begin{array}{cccc}\frac{\partial^2\mathcal{G}}{\partial^2 t_\alpha}\Big|_{(\widetilde{t}^*_\alpha,\widetilde{\tau}^*_\alpha,t_0^*,\tau_0^*)} & \frac{\partial^2\mathcal{G}}{\partial t_\alpha\partial\tau_\alpha}\Big|_{(\widetilde{t}^*_\alpha,\widetilde{\tau}^*_\alpha,t_0^*,\tau_0^*)} & \frac{\partial^2\mathcal{G}}{\partial t_\alpha\partial t_0}\Big|_{(\widetilde{t}^*_\alpha,\widetilde{\tau}^*_\alpha,t_0^*,\tau_0^*)} & \frac{\partial^2\mathcal{G}}{\partial t_\alpha\partial\tau_0}\Big|_{(\widetilde{t}^*_\alpha,\widetilde{\tau}^*_\alpha,t_0^*,\tau_0^*)}\\ \frac{\partial^2\mathcal{G}}{\partial\tau_\alpha\partial t_\alpha}\Big|_{(\widetilde{t}^*_\alpha,\widetilde{\tau}^*_\alpha,t_0^*,\tau_0^*)} & \frac{\partial^2\mathcal{G}}{\partial\tau_\alpha^2}\Big|_{(\widetilde{t}^*_\alpha,\widetilde{\tau}^*_\alpha,t_0^*,\tau_0^*)} & \frac{\partial^2\mathcal{G}}{\partial\tau_\alpha\partial t_0}\Big|_{(\widetilde{t}^*_\alpha,\widetilde{\tau}^*_\alpha,t_0^*,\tau_0^*)} & \frac{\partial^2\mathcal{G}}{\partial\tau_\alpha\partial\tau_0}\Big|_{(\widetilde{t}^*_\alpha,\widetilde{\tau}^*_\alpha,t_0^*,\tau_0^*)}\\ \frac{\partial^2\mathcal{G}}{\partial t_0\partial t_\alpha}\Big|_{(\widetilde{t}^*_\alpha,\widetilde{\tau}^*_\alpha,t_0^*,\tau_0^*)} & \frac{\partial^2\mathcal{G}}{\partial t_0\partial\tau_\alpha}\Big|_{(\widetilde{t}^*_\alpha,\widetilde{\tau}^*_\alpha,t_0^*,\tau_0^*)} & \frac{\partial^2\mathcal{G}}{\partial t_0\partial t_0}\Big|_{(\widetilde{t}^*_\alpha,\widetilde{\tau}^*_\alpha,t_0^*,\tau_0^*)} & \frac{\partial^2\mathcal{G}}{\partial t_0\partial\tau_0}\Big|_{(\widetilde{t}^*_\alpha,\widetilde{\tau}^*_\alpha,t_0^*,\tau_0^*)}\\ \frac{\partial^2\mathcal{G}}{\partial\tau_0\partial t_\alpha}\Big|_{(\widetilde{t}^*_\alpha,\widetilde{\tau}^*_\alpha,t_0^*,\tau_0^*)} & \frac{\partial^2\mathcal{G}}{\partial\tau_0\partial\tau_\alpha}\Big|_{(\widetilde{t}^*_\alpha,\widetilde{\tau}^*_\alpha,t_0^*,\tau_0^*)} & \frac{\partial^2\mathcal{G}}{\partial\tau_0\partial t_0}\Big|_{(\widetilde{t}^*_\alpha,\widetilde{\tau}^*_\alpha,t_0^*,\tau_0^*)} & \frac{\partial^2\mathcal{G}}{\partial\tau_0\partial\tau_0}\Big|_{(\widetilde{t}^*_\alpha,\widetilde{\tau}^*_\alpha,t_0^*,\tau_0^*)}\end{array}\right). \tag{A.18}$$

At the global minimum the disorder averaged partition function becomes

$$\begin{aligned}[\mathcal{Z}^n]_d &= \frac{1}{\mathcal{N}}\int_{-\frac{1}{2}}^{\frac{1}{2}}d^3t_\alpha\int_{-\frac{1}{2}}^{\frac{1}{2}}d^3\tau_\alpha\int_{-\frac{1}{2}}^{\frac{1}{2}}d^3t_0\int_{-\frac{1}{2}}^{\frac{1}{2}}d^3\tau_0\exp\left\{-\mathcal{G}(\widetilde{t}^*_\alpha,\widetilde{\tau}^*_\alpha,t_0^*,\tau_0^*)\right.\\ &- \frac{1}{2}\left(\begin{array}{cccc}t_\alpha-\widetilde{t}^*_\alpha, & \tau_\alpha-\widetilde{\tau}^*_\alpha, & t_0-t_0^*, & \tau_0-\tau_0^*\end{array}\right)F_1\left(\begin{array}{c}t_\alpha-\widetilde{t}^*_\alpha\\ \tau_\alpha-\widetilde{\tau}^*_\alpha\\ t_0-t_0^*\\ \tau_0-\tau_0^*\end{array}\right)\\ &\left.+O(3)\right\}.\end{aligned} \tag{A.19}$$

The normalization factor $\mathcal{N}$ could be expressed as follows,

$$\begin{aligned}\mathcal{N} &= \int_{-\frac{1}{2}}^{\frac{1}{2}} d^3t_0 \int_{-\frac{1}{2}}^{\frac{1}{2}} d^3\tau_0 \exp\left\{-\widetilde{\mathcal{G}}(t_0^*,\tau_0^*) - \frac{1}{2}\begin{pmatrix} t_0, & \tau_0 \end{pmatrix} \widetilde{F_1} \begin{pmatrix} t_0 \\ \tau_0 \end{pmatrix} + O(3)\right\}. \\ &= \exp\left(-\widetilde{G}(t_0^*,\tau_0^*) - \frac{1}{2}\ln\det\widetilde{F_1}\right) \end{aligned} \tag{A.20}$$

where

$$\widetilde{F_1} = \begin{pmatrix} \frac{\partial^2\widetilde{\mathcal{G}}}{\partial t_0^2}\mid_{(t_0^*,\tau_0^*)} & \frac{\partial^2\widetilde{\mathcal{G}}}{\partial t_0\partial\tau_0}\mid_{(t_0^*,\tau_0^*)} \\ \frac{\partial^2\widetilde{\mathcal{G}}}{\partial\tau_0\partial t_0}\mid_{(t_0^*,\tau_0^*)} & \frac{\partial^2\widetilde{\mathcal{G}}}{\partial\tau_0^2}\mid_{(t_0^*,\tau_0^*)} \end{pmatrix}, \tag{A.21}$$

with

$$\widetilde{\mathcal{G}} = \frac{3}{2}\ln(3+\beta k R_0^2(1-2t_0^2-2\tau_0^2)) + \frac{3}{2}\,\mathrm{Tr}\ln(\widetilde{M_0}). \tag{A.22}$$

Now the disorder averaged partition function could be expressed as follows

$$[\mathcal{Z}^n]_d = \frac{1}{\mathcal{N}}\exp\left(-\widetilde{\mathcal{G}}(t_0^*,\tau_0^*,t_0^*,\tau_0^*) - \frac{1}{2}\ln(\det F_1)\right).$$

Getting elements of F_1 is a very tedious process. However, we anticipate that for small motor force, this is practical calculation to do. We expect that in addition to the elastic response this will yield corrections to the elastic response depending on the motor force and ratio of the spring constant of the chain to the spring constant of the motor.

Bibliography

[1] B. Alberts, D. Bray, J. Lewis, M. Raff, K. Roberts, and J. D. Watson. *Molecular Biology of The Cell*. Garland Publishing, inc. New York and London, 1989.

[2] R. Alexander-Katap and S. F. Edwards:. The statistical mechanics of entangled polymers. *J. Phys. A*, 5:674, 1972.

[3] F. Backouche, L. Haviv, D. Groswasser, and A. Bernheim-Groswasser. Active gels: dynamics of patterning and self-organization. *Phys. Biol.*, 3:264273, 2006.

[4] R. C. Ball, M. Doi, S. F. Edwards, and M. Warner. Elasticity of entangled networks. *Polymer*, 22:1010–1018, 1981.

[5] J. Colombelli, A. Besser, H. Kress, E.G. Reynaud, P. Girard, E. Caussinus, U. Haselmann, J.V Small, U.S Schwarz, and E.H Stelzer. Mechanosensing in actin stress fibers revealed by a close correlation between force and protein localization. *Journal of Cell Science, 1928*, 122:1665–1679, 2009.

[6] R. T. Deam and S. F. Edwards. The theory of rubber elasticity. *Proceedings of the Royal Society*, 280:317–353, 1976.

[7] M. Doi and S. F Edwards. *The Theory of Polymer Dynamics*. Clarendon Press Oxford, 1986.

[8] M. Doi and H. See. *Introduction to Polymer Physics*. Clarendon Press Oxford, 1996.

[9] K. Doubrovinski and K. Kruse. Self-organization in systems of treadmilling filaments. *The European Physical Journal E*, 31(1):95–104, 2010.

[10] S. F. Edwards and P. W. Anderson. Theory of spin glasses. *J. Phys.*, 5:965–974, 1975.

[11] S. F. Edwards and K. K Müller-Nedebock. Entanglements in polymers: II networks. *J. Phys. A: Math. Gen.*, 32:33013320, 1099.

[12] S. F. Edwards and T. A. Vilgis. The tube model theory of rubber elasticity. *Rep. Prog. Phys.*, 51:243–297, 1988.

[13] P. J. Flory. Molecular theory of rubber elasticity. *Polymer*, 20:1317–1319, 1979.

[14] M. L. Gardel, I. C. Schneider, Y. Aratyn-Schaus, and C. M. Waterman. Mechanical integration of actin and adhesion dynamics in cell migration. *Annu. Rev. Cell Dev. Biol.*, 26:315333, 2010.

[15] T. E. Holy and S. Leibler. Dynamic instability of microtubules as an efficient way to search in space. *Proc. Natl. Acad. Sci. USA*, 91:5682, 1994.

[16] S. Honore, E. Pasquier, and D. Braguer. Understanding microtubule dynamics for improved cancer therapy. *Cellular and Molecular Life Sciences*, 62:3039 – 3056, 2005.

[17] A. F. Huxley. Mechanics and models of the myosin motor. *Phil. Trans. R. Soc. Lond. B*, 355,:433–440, 2000.

[18] P. A. Janmey. The cytoskeleton and cell signaling: Component localization and mechanical coupling. *Physiological Reviews*, 78:763–781, 1998.

[19] F. Jülicher, A. Ajdari, and J. Prost. Modeling molecular motors. *Rev.,Mod.,Phys.,*, 69:1270–1281, 1997.

[20] F. Jülicher, K. Kruse, J. Prost, and J.-F Joanny. Active behavior of the cytoskeleton. *Physics Reports*, 449:3–28, 2007.

[21] G. Karp. *Cell and Molecular Biology concepts and Experiments*. John Wiley and Sons, Inc., 2008.

[22] S. Kim and A. P. Coulombe. Emerging role for the cytoskeleton as an organizer and regulator of translation. *Nat. Rev. Mol. Cell. Biol.*, 11:1471–0072, 2010.

[23] K. Kruse, J. F. Joanny, F. Jülicher, J. Prost, and K. Sekimoto. Asters, vortices, and rotating spiral in active gels of polar filaments. *Phy. Rev. Lett.*, 92:0781011–0781014, 2004.

[24] K. Kruse, J.F. Joanny, F. Jülicher, J. Prost, and J.K. Sekimoto. Generic theory of active polar gels: a paradigm for cytoskeletal dynamics. *Eur. Phys. J. E*, 16(1):5–16, 2005.

[25] F. Lautenschlager, S. Paschke, S. Schinkinger, A. Brueld, M. Beil, and J. Guck. The regulatory role of cell mechanics for migration of differentiating myeloid cells. *PNAS*, 106:15696 15701, 2009.

[26] T. B. Liverpool, M. C. Marchetti, J. F. Joanny, and J. Prost. Mechanical response of active gels. *Europhysics Letters*, 85:18007, 2009.

[27] C. A. Parent. Making all the right moves: chemotaxis in neutrophils and dictyostelium. *Current Opinion in Cell Biology*, 16(1):4–13, 2004.

[28] M. Rubinstein and S. Panyukov. Elasticity of polymer networks. *Macromolecules*, 35:6670–6686, 2002.

[29] P. Sotta and B. Deloche. Uniaxiality induced in a strained poly(dimethylsi1oxane) network. *Macromolecules*, 1990:1999–2007, 23.

[30] J. Stricker, F. Tobias, and G. L. Margaret. Mechanics of the f-actin cytoskeleton. *Journal of Biomechanics*, 43(1):9–15, 2010.

[31] T. Surrey, F. Nedelec, S. Leibler, and E. Karsenti. Physical properties determining self-organization of motors and microtubules. *Science*, 292:1167–1171, 2001.

[32] T. Surrey, F. Nedelec, S. Leibler, and E. Karsenti. Self-organization of motors and microtubules. *Science*, 292:1167–1171, 2001.

[33] L. R. G. Treloar. *The Physics of Rubber Elasticity.* Oxford: Clarendon Press, 1975.

[34] F. W. Wiegel. *Introduction to Path integral Methods in Physics and Polymer Science.* Philadelphia: World Scientific, 1896.

[35] M. Yu, M. Yuan, and H. Ren. Visualization of actin cytoskeletal dynamics during the cell cycle in tobacco (nicotiana tabacum l. cv bright yellow) cells. *Biol. Cell,*, 98:295306, 2006.

[36] K. B. Zeldovich, J.-F. Joanny, and J. Prost. Motor protain transporting cargos. *The European Physical Journal E*, 70:155–163, 2004.